Cold Regions Science and Technology 57 (2009) 67–90

Contents lists available at ScienceDirect

Cold Regions Science and Technology

journal homepage: www.elsevier.com/locate/coldregions

Iceberg drift modelling and validation of applied metocean hindcast data

Kenneth Eik *

Norwegian University of Science and Technology, Norway
StatoilHydro, Trondheim, Norway

ARTICLE INFO

Article history:
Received 5 November 2008
Accepted 21 February 2009

Keywords:
Iceberg drift
Hindcast validation
Barents Sea

ABSTRACT

An iceberg drift model covering the Barents and Kara Seas has been developed. The skills of the model relies both on the ability to describe physical actions from the environment on the icebergs and the accuracy of the applied metocean variables (wind, waves and currents). Experiences from the East Coast of Canada show that iceberg modelling may work reasonably well and indicate that iceberg drift models are able to fulfil both of the above mentioned requirements. By applying similar models in other regions, it may be assumed that wind, waves and currents affect the iceberg in a similar way as at the East Coast of Canada. However, the reliability of available metocean data sources will vary significantly from region to region. Due to this, a study with the objective to evaluate the quality of the underlying metocean models has been performed.

A significant amount of recorded wind, wave and current data from various regions in the Barents Sea have been applied in comparisons with hindcast data from selected atmospheric and oceanographic models. Results show that the quality of wind and wave data applied by the iceberg drift model is very good. Regarding current velocity, there is a poor match between data from the applied oceanographic model and measurements. A method for improving the current magnitude has been introduced.

The relative importance of winds, waves and currents on iceberg drift has also been investigated. In general, currents are most important for iceberg drift. However, in open waters, the wave drift may become the most important forcing. The presented iceberg drift model is considered to provide good results in situations with strong winds (and waves) and low currents while situations with low winds will give less reliable results. It is concluded that the quality of incorporated metocean data in any iceberg drift model need to be documented in order to fully understand possible limitations in iceberg drift simulations. Further work should focus on improvements in oceanographic modelling in order to establish a more reliable oceanographic hindcast for the Barents Sea.

1. Introduction

Searching for oil and gas in regions infested by sea ice and icebergs has been ongoing for several decades. Considering the increasing price for hydrocarbons during the recent years and a suggestion by the US Geological Survey that 25% of the remaining hydrocarbon resources in the world are located in the arctic, a strong increase in arctic offshore activities must be expected.

As offshore activities are moving northwards the presence of icebergs in some areas will affect both designs of new installations as well as plans for marine operations. Knowledge regarding frequency and characteristics of icebergs will be crucial in order to ensure safe and efficient operations. During the recent decades, a number of iceberg drift models have been presented for various regions and one of these models is presently used operationally with great success offshore the East Coast of Canada (Kubat et al., 2005). However, common for most of the published models, is an insufficient validation of the underlying atmospheric and oceanographic model skills. The validations are typically limited to some few comparisons between iceberg drift trajectories from the model and from physical recordings. In order to get the proper understanding regarding why (or why not) the iceberg drift model gives a good description of the physical iceberg drift, it is proposed to perform validation studies of the oceanographic and atmospheric models that provide input to the iceberg drift model. The validations include comparisons between modelled and measured metocean data both over large geographical areas as well as over a relatively long time period.

This paper presents an iceberg drift model valid for the Barents Sea (Fig. 1) and the basic metocean models that it is based on. The objective has been to establish tools to evaluate model quality both with respect to directionality as well as strength in wind, current

* Fax: +47 73 59 70 21.
E-mail address: kenjo@statoilhydro.com.

0165-232X/$ – see front matter © 2009 Elsevier B.V. All rights reserved.
doi:10.1016/j.coldregions.2009.02.009

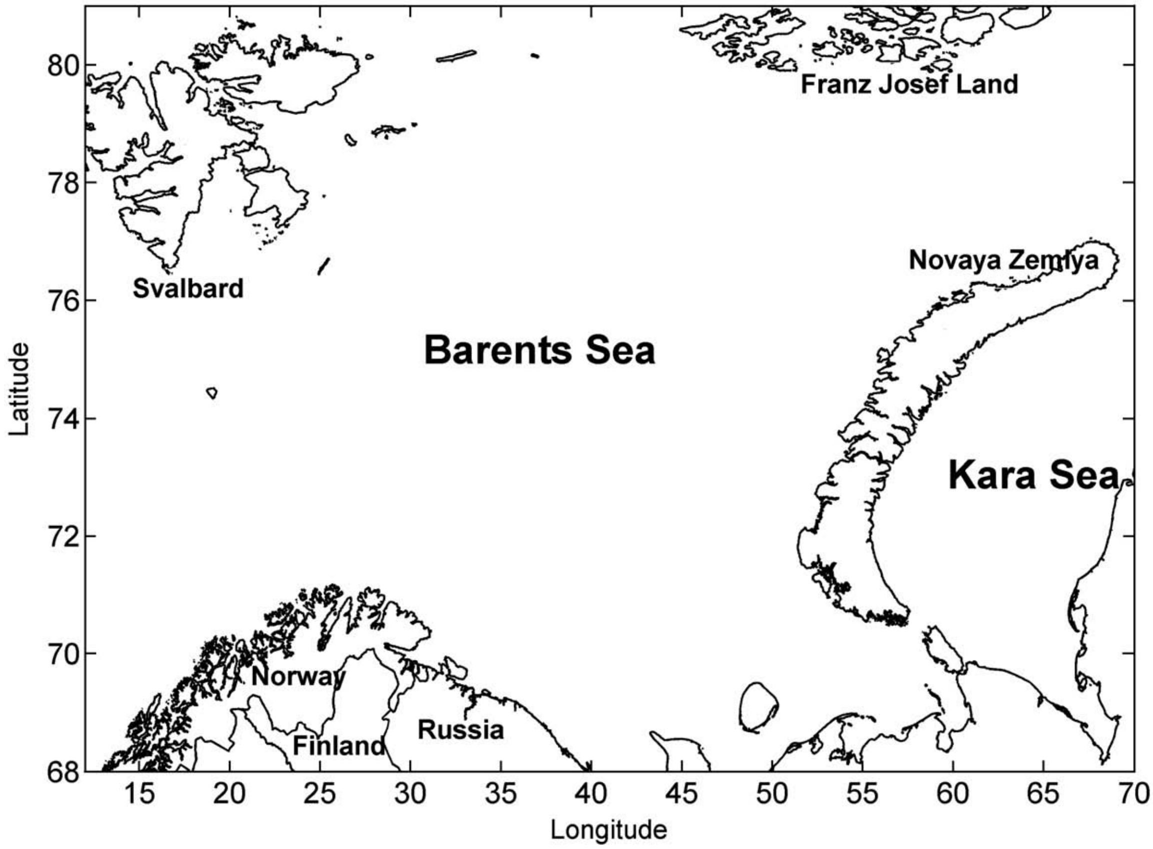

Fig. 1. Map showing the region covered by the iceberg drift model.

and waves. A methodology for improving current data has also been introduced. Finally, a comparison between iceberg drift trajectories from model and from physical recordings has been included.

The model evaluations are followed by a discussion regarding results and the methodology that has been applied. Conclusions are drawn based on the results and recommendations for future work are highlighted.

2. Iceberg drift model

The iceberg drift model presented in this paper is basically an update version of the iceberg drift model presented by Johannessen et al. (1999).

2.1. Momentum balance

To find the movement of an iceberg in an initially known position, we integrate the speed that the iceberg is moving with. To find the speed we integrate the acceleration given by Newton's 2. law:

$$m\frac{d\mathbf{V}_\mathrm{i}}{dt} = -mf\mathbf{k}\times\mathbf{V}_\mathrm{i} + \mathbf{F}_\mathrm{a} + \mathbf{F}_\mathrm{w} + \mathbf{F}_\mathrm{wd} + \mathbf{F}_\mathrm{si} + \mathbf{F}_\mathrm{p} \quad (1)$$

where $m = m_0(1 + C_m)$ and m_0 is the physical mass and C_m is the coefficient of added mass. V_i is the local velocity of the iceberg, $-\mathbf{fk}\times\mathbf{V}_i$ is the Coriolis parameter and k is the unit vector in vertical direction. Further, $\mathbf{F}_\mathrm{a,w}$ is the air and water form drag, respectively. $\mathbf{F}_\mathrm{wd}$ is the mean wave drift force, $\mathbf{F}_\mathrm{si}$ is the sea-ice drag and $\mathbf{F}_\mathrm{p}$ is the horizontal gradient force exerted by the water on the volume that the iceberg displaces.

2.2. Numerical integration

The momentum balance of the iceberg is given by Eq. (1). On the basis of Eq. (1) the iceberg drift track $x_i(t)$ is determined by solving the two following coupled differential equations:

$$\frac{dx_i}{dt} = (\mathbf{V}_\mathrm{i} - \mathbf{V}_\mathrm{w}) + \mathbf{V}_\mathrm{w} \quad (2)$$

$$m\left(\frac{d(\mathbf{V}_\mathrm{i} - \mathbf{V}_\mathrm{w})}{dt}\right) = -mf\mathbf{k}\times(\mathbf{V}_\mathrm{i} - \mathbf{V}_\mathrm{w}) + \mathbf{F}_\mathrm{a} + \mathbf{F}_\mathrm{res} + \mathbf{F}_\mathrm{tc} + \mathbf{F}_\mathrm{wd} + \mathbf{F}_\mathrm{si} \quad (3)$$

with given initial conditions, i.e. start position and start velocity. Note that all drag forces on the right-hand side of Eq. (3) are expressed as functions of relative velocities and that the difference between iceberg and water velocity is considered as the unknown variable. F_res is the drag force from residual (weekly averaged) current while F_tc is the drag force from tidal current. Further, the water velocity V_w is found by adding the residual current, V_res and tidal current, V_tc.

Eqs. (2) and (3) are decomposed into two directions, north-south and east-west, and that gives a system of four equations with four unknown variables. The system is solved with the Matlab ODE15S solver (The Mathworks, 2008). This function is called with intervals equal to a time step until specified simulation time is reached.

Table 1
Metocean models included in the iceberg drift model.

Model	Parameters	Sampling	Name	Period	Reference
Coupled ice/oceanographic model	Current velocity Water temperature Salinity Ice velocity Ice thickness Ice concentration Sea surface height	1 week	NERSC Barents Sea model	1987–1992	Keghouche et al. (2007)
Tidal model	Tidal surface elevation Tidal current velocities	Flexible	Tidal model	NA	Gjevik et al. (1994)
Coupled wave/atmospheric model	Wind velocity Wave heights Wave periods Wave direction	6 h	Winch model	1955–2006	Reistad and Iden (1998)

Selection of time step is flexible but usually 2 h are considered adequate. The initial iceberg velocity is set equal to the residual current at the initial iceberg position.

Wind and current forces are described as drag forces and expressions are found in Bigg et al. (1997). Mean wave drift force depends on the icebergs capability to generate waves. Potential theory has been applied in the iceberg drift model. The total fluid velocity potential is written as the sum of encountered and diffracted potential. This approach is justified by making the following assumptions:

- Iceberg velocity and oscillations are small so radiation effects can be neglected.
- Wavelengths are small compared to the iceberg.
- Iceberg walls are vertical so all the encountered waves are reflected.
- Viscous effects are neglected.

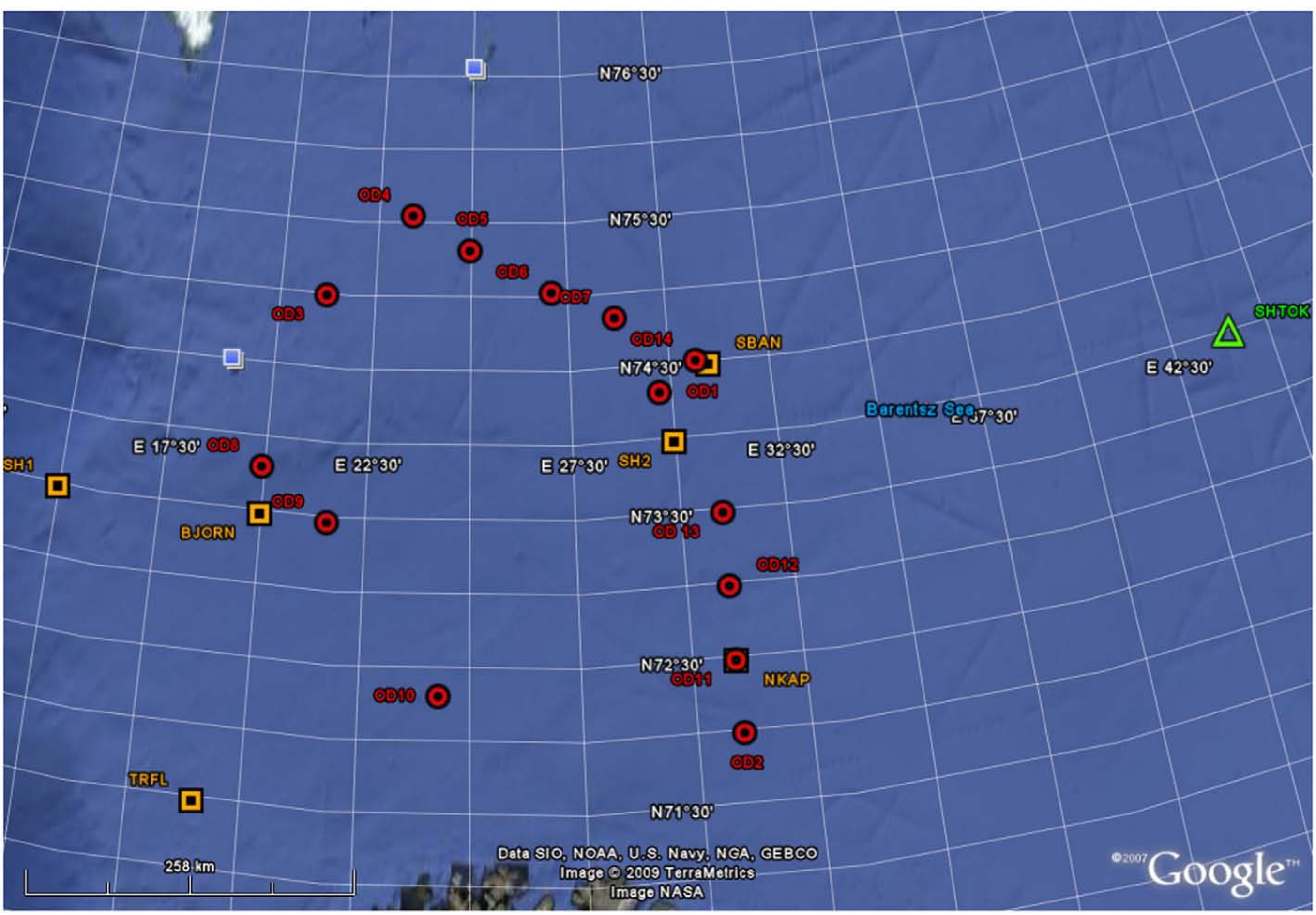

Fig. 2. Map showing locations for current, wave and wind recordings in the Barents Sea. Current recordings are marked with red circles while wind and wave recordings are marked with orange squares. Wind, wave and current recordings are available from the Shtokman location (green triangle). (For interpretation of the references to color in this figure legend, the reader is referred to the web version of this article.)

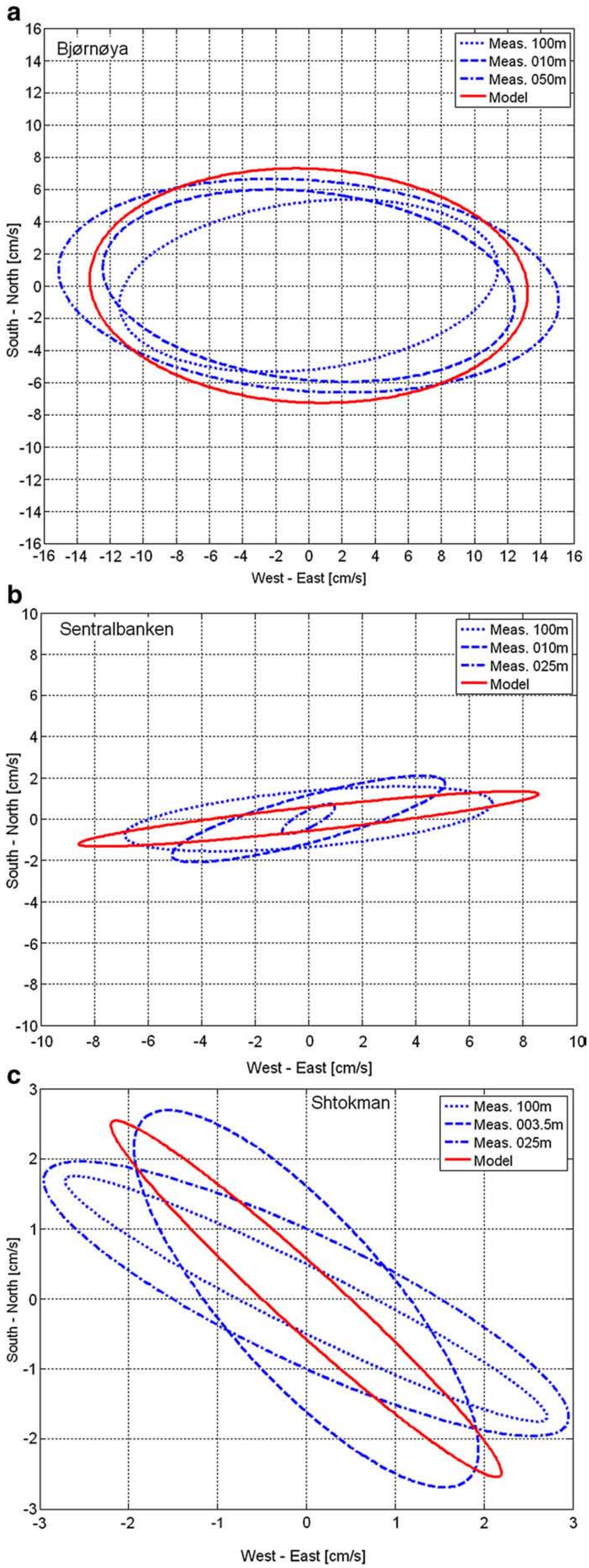

Fig. 3. Tidal ellipses representing M2 from Bjørnøya (a), Sentralbanken (b) and Shtokman (c). The model currents (red circles) are averaged over the entire water column at the location. (For interpretation of the references to color in this figure legend, the reader is referred to the web version of this article.)

In order to take into account, that not all these assumptions are perfectly fulfilled, the wave drift force is multiplied with a wave drift coefficient, C_w. This factor will in general depend on ratios between parameters such as iceberg characteristic length, iceberg draft, wave length and water depth (Isaacson, 1988). In the present iceberg drift model, a constant value has been applied for C_w. Expressions for all forces in the model are presented in Appendix A.

Expression for sea-ice loads on iceberg is based on recommendations from Lichey and Hellmer (2001). In general, in moderate ice concentrations, the sea-ice force is considered as a drag-type force where the relative velocity between iceberg drift speed and sea-ice drift speed is applied. For high ice concentrations (more than 90%) combined with sufficiently thick ice, the iceberg is locked into the sea ice and follows the sea-ice drift. Forces from waves and sea ice are not allowed to act simultaneously. For ice concentrations less than 15%, force from sea ice is set to zero. For ice concentrations up to 40%, sea ice force is included only if there are no waves. For ice concentrations above 40%, wave drift forces are omitted. All expressions including recommended values for all required parameters are presented in Appendix A.

3. Data sources

3.1. Model data

A summary of the metocean data models that have been used to generate input to the iceberg drift model are given in Table 1. More detailed information on the models are presented in Sections 3.1.1–3.1.3.

3.1.1. Coupled ice and oceanographic model

Presently, several ice and oceanographic models covering the Barents and Kara Seas have been established by international recognised institutes such as the Nansen Environmental and Remote Sensing Center (NERSC), the Arctic and Antarctic Research Institute (AARI) and the Norwegian Meteorological Institute (met.no). However, none of these models have been used to generate a complete long term hindcast archive which is required by the iceberg drift model. Due to this, NERSC was contracted by StatoilHydro in 2006 in order to establish an ice/ocean hindcast archive covering the period 1987 to 1992 continuously. The NERSC Barents Sea model was used to generate weekly averaged values for current at 3, 10, 50 and 100 m depths and sea ice with a grid resolution of 10 km.

The ocean velocities provided by NERSC are based on a model system consisting of an improved version of the Hybrid Coordinate Ocean Circulation Model (HYCOM) coupled to a sea-ice model based on Elastic Visco Plastic rheology. The model system use ERA-40 atmospheric forcing from the European Center for Medium range Weather Forecasting (ECMWF) and boundary conditions given by the TOPAZ forecasting system for the Atlantic and Arctic Oceans. Details and references on the models are found in Keghouche et al. (2007).

In the iceberg drift simulation model, the currents from the four levels are averaged over the depth of the iceberg.

3.1.2. Tidal model

The tidal potential is usually described by a sum of several periodic elements and may be used for predictions of tidal currents. The tidal

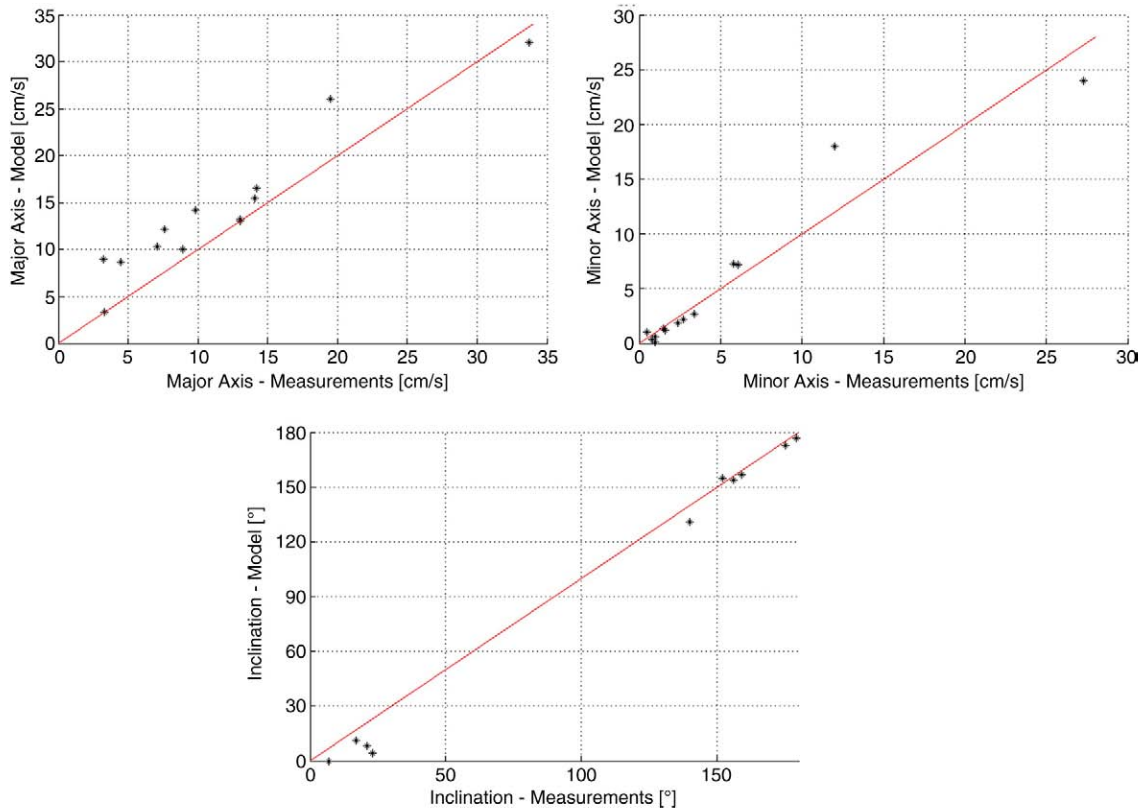

Fig. 4. Comparisons of tidal constituent M2 from tidal current model (Gjevik and Straume, 1998) and measurements (Oceanor, 1998). M2 is specified by magnitude of major axis (upper left), minor axis (upper right) and inclination (lower left). Each dot corresponds to data from an oceanographic station (ref. Appendix B).

model used in the iceberg drift model is described in Gjevik et al. (1994) and provides information on four of the most common periodic constituents; M2, N2, S2 and K1. Both M2 and N2 are due to gravity forces from the moon while S2 is caused by the sun. Forcing from these three constituents is repeated twice per day. K1 is caused by both the sun and the moon and has a diurnal period. In the iceberg drift model, tidal currents, which have been generated from these constituents, have been superposed on the weekly averaged currents from the oceanographic model (Keghouche et al., 2007). The tidal currents in the iceberg drift model are averaged over the entire water depth.

3.1.3. Coupled wave and atmospheric model

In similarity to the oceanographic models, several meteorological and wave models have been developed for all or parts of the Barents and Kara Seas. As input to the iceberg drift model, it was decided to use the Winch hindcast archive developed by the Norwegian Meteorological Institute (Reistad and Iden, 1998). The wind/wave hindcast archive were selected as it provides a uniquely long data set (1955–2006) that covers both the Barents and the Kara Seas with a grid resolution of 1.5°×0.5° East/West and North/South respectively. Sampling interval is 6 h. A second reason for selecting this hindcast to the iceberg drift model was that historical comparisons with data from this model and wind/wave recordings from the North Sea and the Norwegian Sea have documented fairly good quality on the model data.

With respect to winds, the model calculates geostrophic winds based on gridded mean sea level pressure data. A two layered boundary layer model is applied to derive 10 m wind based on the geostrophic wind. Surface roughness over sea has been applied for the entire model domain thus reliability of winds over sea ice and land is reduced compared to winds over open water.

With respect to waves, the Winch model is a deep water discrete wave prediction model developed by Oceanweather Inc. and run by the meteorological institute. The propagation scheme is a downstream advection scheme. The wave spectrum is divided into 24 direction bands with 15° bandwidth and 15 frequency bands ranging from 0.04 Hz to 0.24 Hz. The parametric wave growth is derived from empirical fetch limited growth data and forces the wind sea to conform to a reference spectrum of the JONSWAP type. The fetch will depend on the ice conditions thus monthly average ice borders have been applied in the model. If ice concentration in a grid point is less than 40% the grid point is treated as open water in the wave model. If the ice concentration is higher than 40% the wave energy has been set to zero.

Details on the model and references on the Winch model are found in Reistad and Iden (1998).

Table 2
Validation studies and intention with study.

Comparison		Purpose
1	Time series	Indicates differences in magnitude and whether physical variations have been captured by the model
2	Scatter plot of current magnitudes	Shows potential bias in model data and visualise uncertainties in the model
3	Quantile–Quantile (QQ) plots	Shows potential bias in model data. Compares values at different statistical levels (quantiles) from model and measurements.
4	Directional distributions	Shows potential bias in directionality in model data
5	Trajectories	Illustrates the skills of the model with respect to use in an iceberg drift model.

3.2. Measured data

3.2.1. Current recordings

Measured currents from water depths 3, 10, 25, 50 and 100 m from 12 different sites in the Norwegian part of the Barents Sea and from the Shtokman site in the Russian sector of the Barents Sea have been used in the validation of model data. The locations are presented in the map shown in Fig. 2. The recordings from the Norwegian sector come from an initiative by the Norwegian Petroleum Directorate (NPD) in the eighties and are reported by Oceanor (1998). Recordings from the Shtokman field were carried out by Oceanor in the period 1992–1997 and were reported by Kleiven and Meisingset (2003). Presently, recordings from the Shtokman field are not publicly available. Time spans of Barents Sea current measurements applied in this study are presented in Appendix B.

3.3. Wind and wave recordings

As for the currents, the majority of available wind and wave recordings are available thanks to the NPD initiative in the eighties. Both various buoys as well as meteorological vessels (AMI and Endre Dyrøy) were used in the data acquisition programme. In this study, recordings from Tromsøflaket, Bjørnøya, Nordkappbanken and Sentralbanken have been applied (Oceanor, 1998). In addition, wind and wave recordings from buoys at Shtokman have been applied (Kleiven and Meisingset, 2003). Finally, wind and wave data have been collected at two locations from 2007 after an initiative by StatoilHydro. These data are also applied in this study, despite that data yet not have been reported. All locations are shown in Fig. 2 while time spans for the recordings are presented in Appendix B.

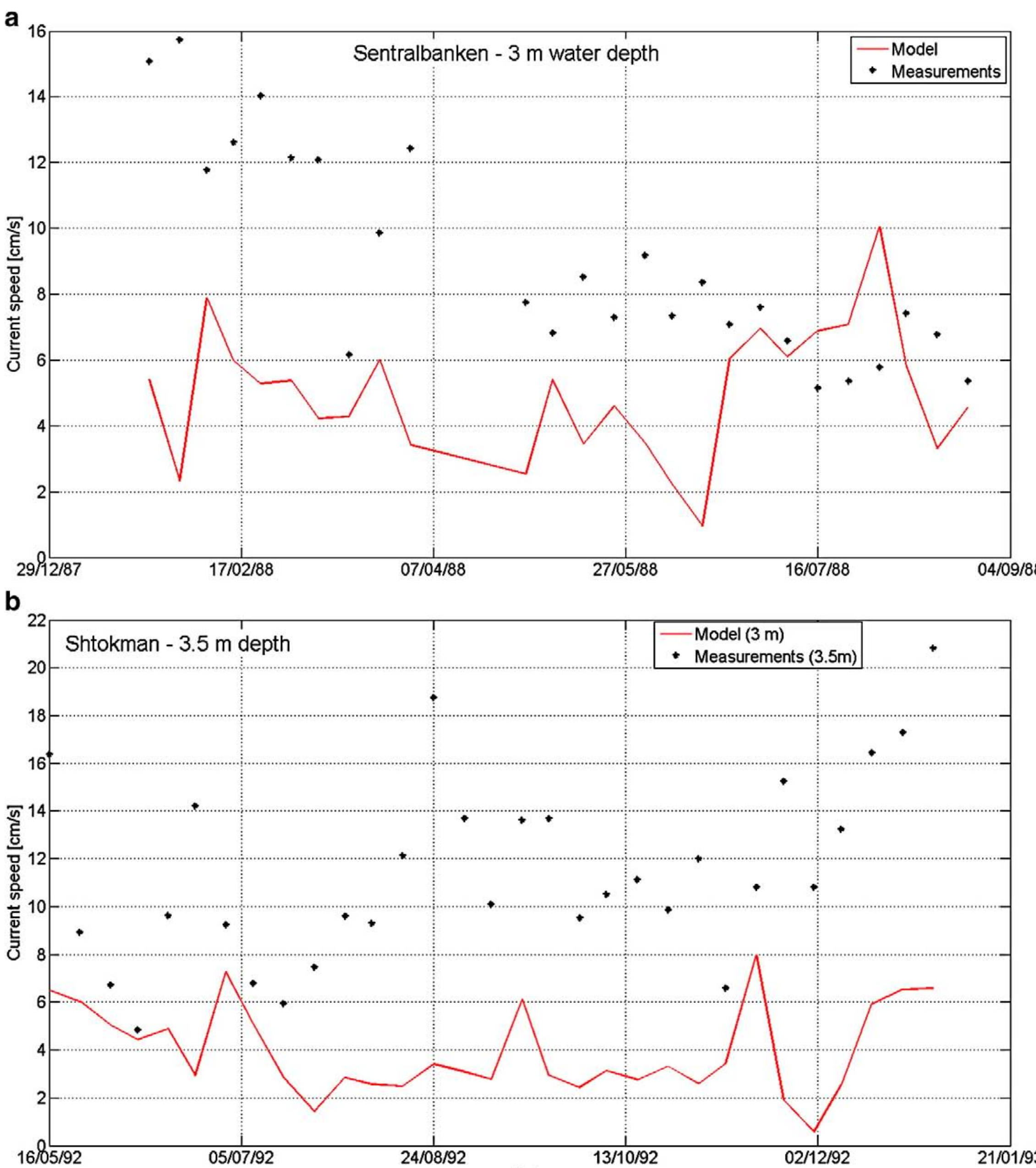

Fig. 5. Time series of measured and model current speed from Sentralbanken (a and c) and from Shtokman (b and d) at 3 and 100 m depth respectively.

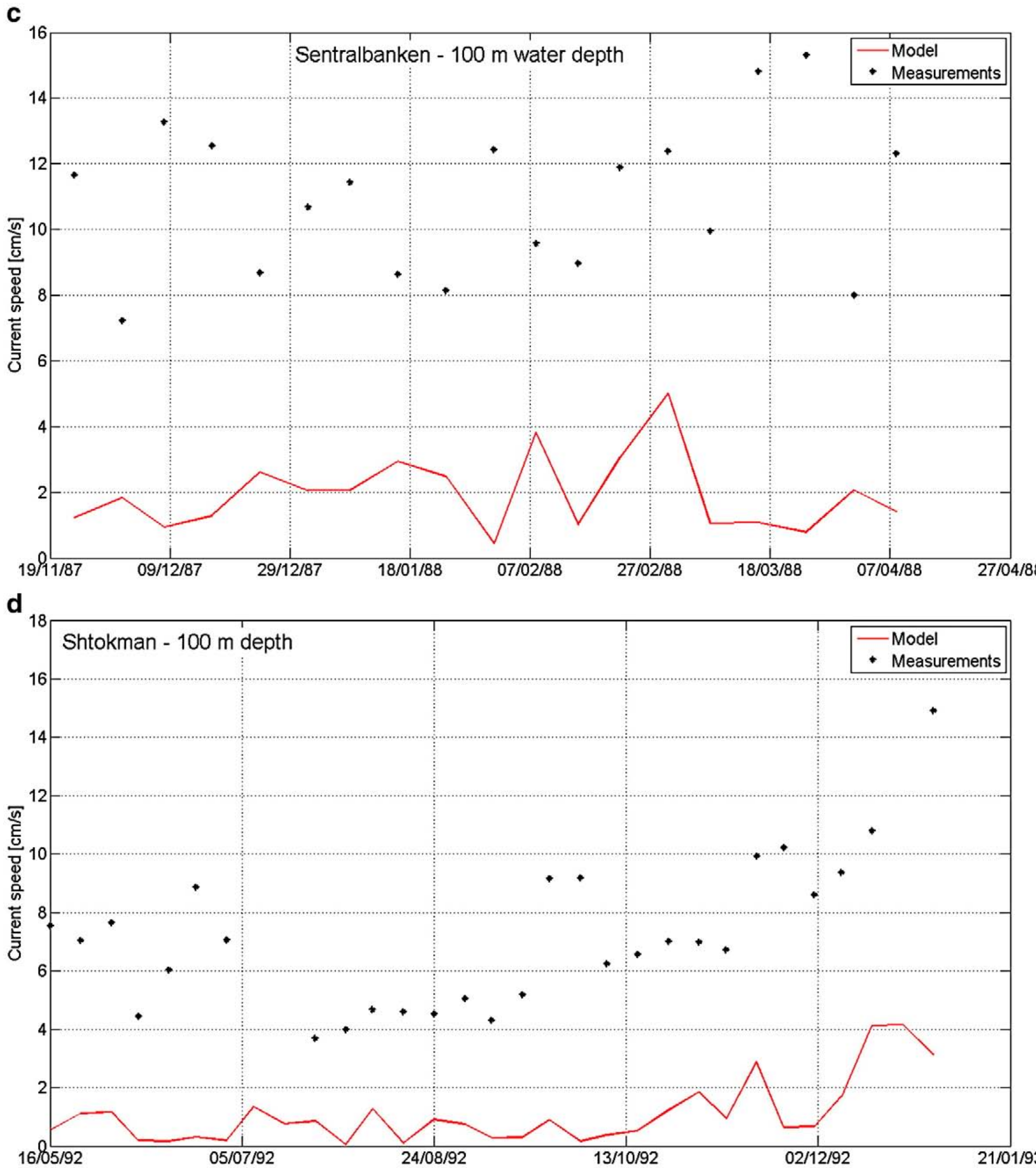

Fig. 5 (*continued*).

3.3.1. Iceberg trajectories

During the Ice Data Acquisition Program (IDAP) 1988–1994, totally 53 drift buoys were deployed on icebergs (Spring, 1994). Data from these buoys were filtered and smoothed to hourly sampled time series. Of these trajectories, 26 have been stored in the StatoilHydro database and are applied in these studies. It should be noted however, that a number of these trajectories show that a large number of the icebergs were grounded for long periods thus not particularly suited for validation of the iceberg drift model. Other iceberg trajectories have been excluded from the study due to lack of knowledge regarding the iceberg size and geometry. Remaining icebergs (7) have been used in comparisons with model trajectories.

Two iceberg trajectories were also recorded close to Franz Josef Land and Novaya Zemlya respectively by the Arctic and Antarctic Research Institute (AARI) in 2005 (Dmitriev and Nesterov, 2007). Both these trajectories have been included in the validation studies.

4. Validation studies

4.1. Oceanographic validations

As the currents applied in the iceberg drift model come from two different models, the validation is split into two different types of analyses. With respect to tidal currents, comparisons of four constituents (M2, N2, S2 and K1) from tidal model and measurements are carried out. With respect to weekly averaged currents, simultaneous currents from measurements and oceanographic model are compared both with respect to magnitude and directionality.

4.1.1. Tidal currents

Harmonic analyses have been performed with data from all oceanographic stations listed in Appendix B. The Harmonic analyses have been done in accordance with software and recommendations published by Foreman (1978). In total, 60 constituents are estimated by the harmonic analyses. However, only four constituents are included in the tidal model, thus only M2, N2, S2 and K1 have been included in the validations. It has previously been reported that M2 and K1 are the major diurnal and semidiurnal constituents in the Barents Sea (Gjevik and Straume, 1998). With respect to magnitude of the major axis in the tidal ellipses, the harmonic analyses showed that M2 in general is approximately twice as high as any of S2, N2 and K1. Due to this, results only for M2 are presented in this paper. However, it should be noted that results for the other constituents show similar trends as for M2.

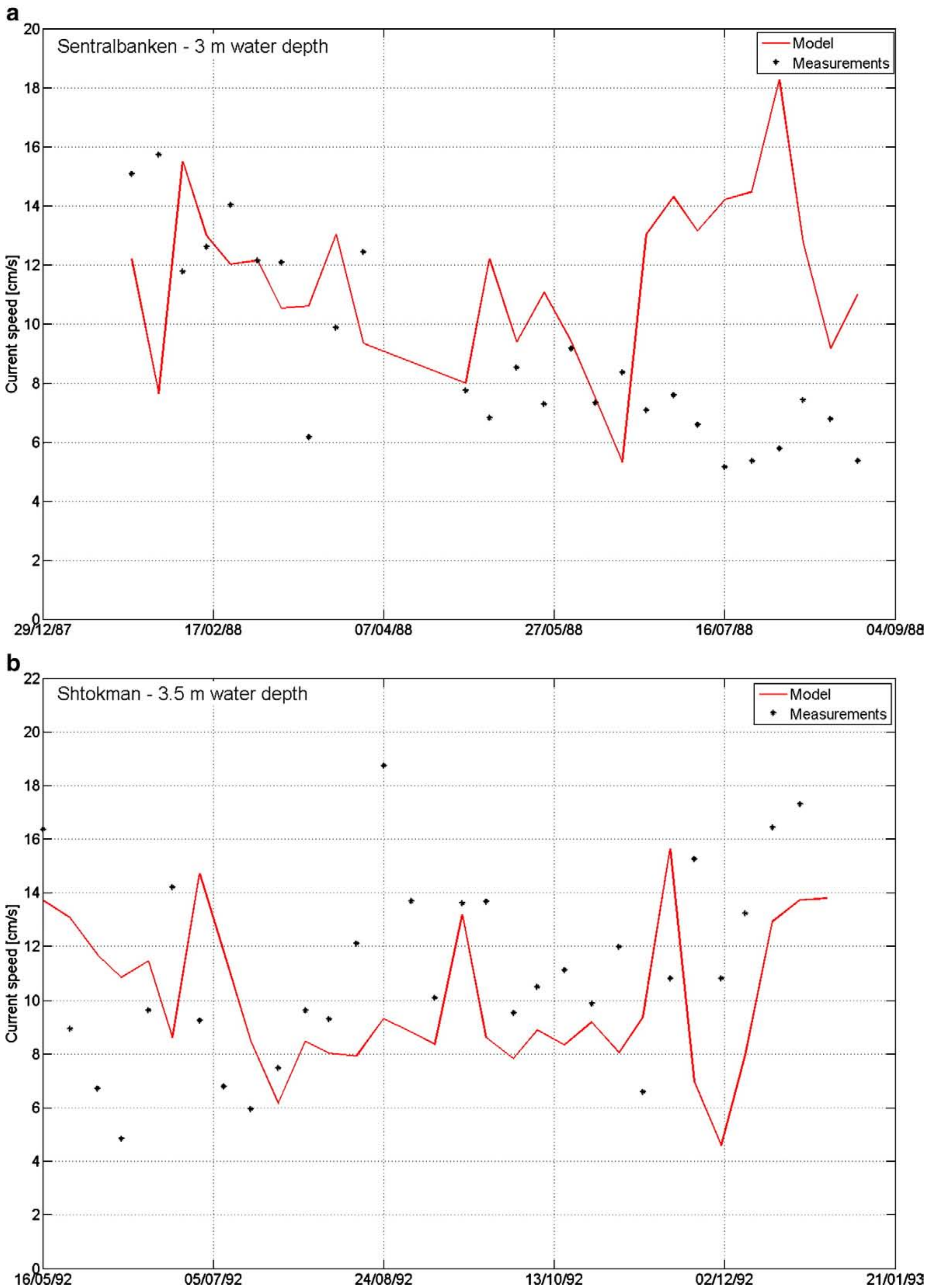

Fig. 6. Time series of measured and modified model current speed from Sentralbanken (a and c) and from Shtokman (b and d) at 3 and 100 m depth respectively.

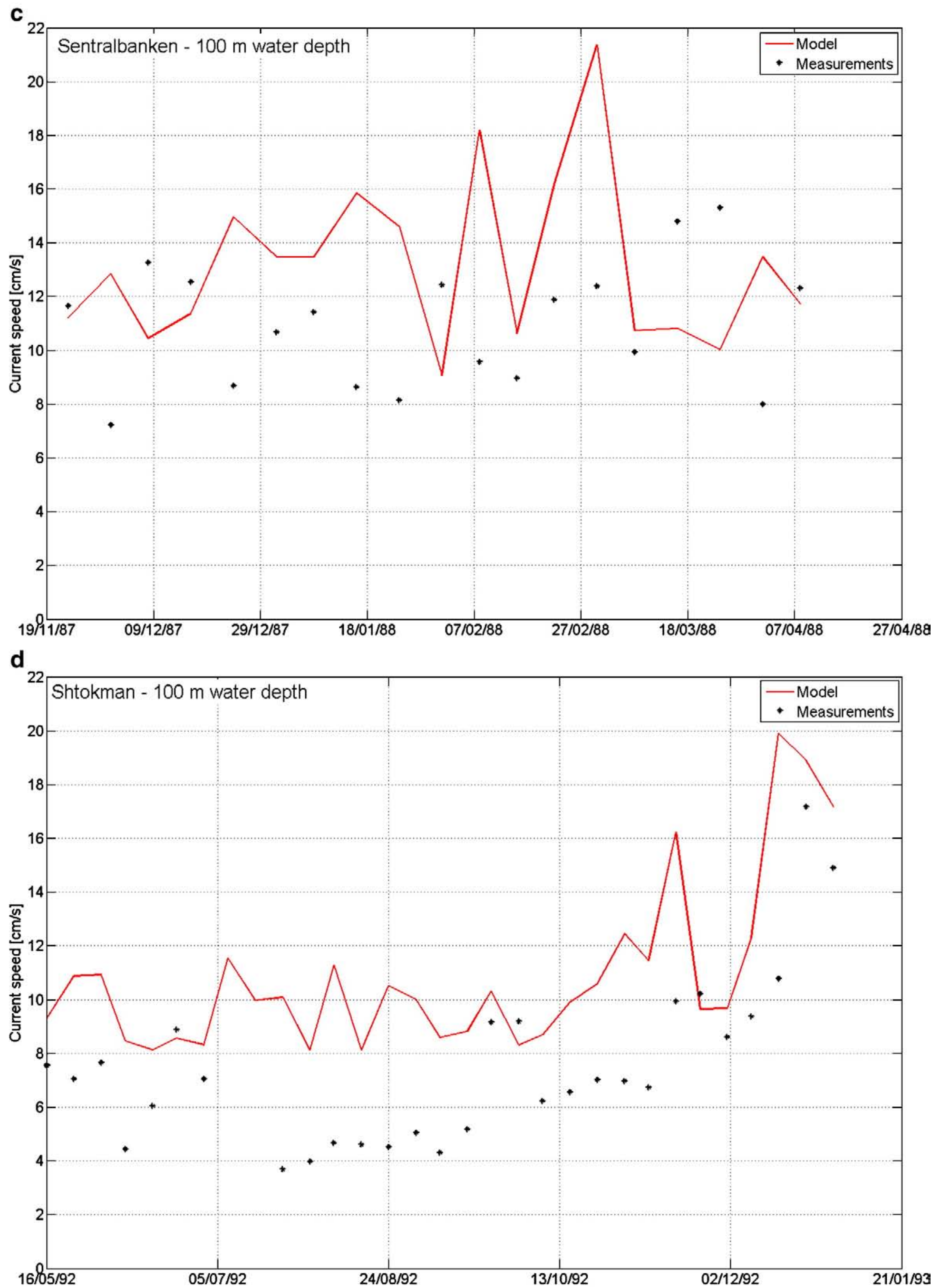

Fig. 6 (*continued*).

Tidal ellipses have been drawn for all locations and plots including ellipses from both measurements and model have been generated. These ellipses comprise information regarding magnitude and direction of currents caused by the constituents. As the model generates a depth averaged current, only one ellipse represents the model at each site. With respect to measurements, ellipses based on data from 10 m, 25 m and 100 m depths have been drawn. Fig. 3 shows the comparisons of ellipses from Bjørnøya, Sentralbanken and Shtokman for the constituent M2. The locations are denoted OD8, OD7 and SHTOK in Fig. 2. Fig. 4 shows scatter diagrams comparing M2 major

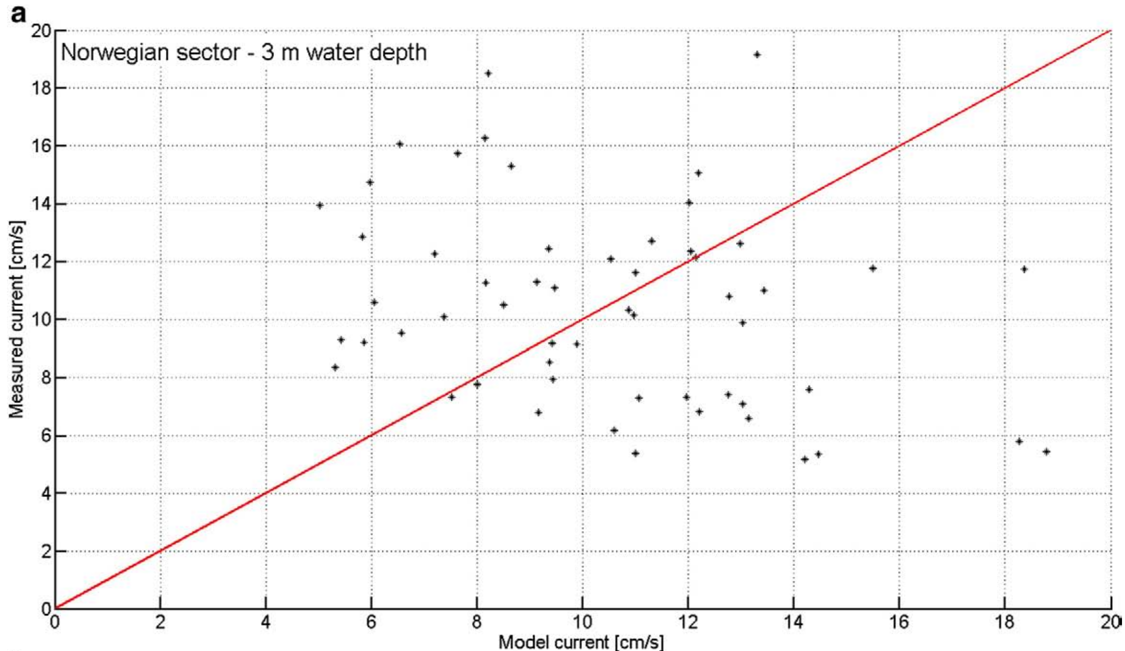

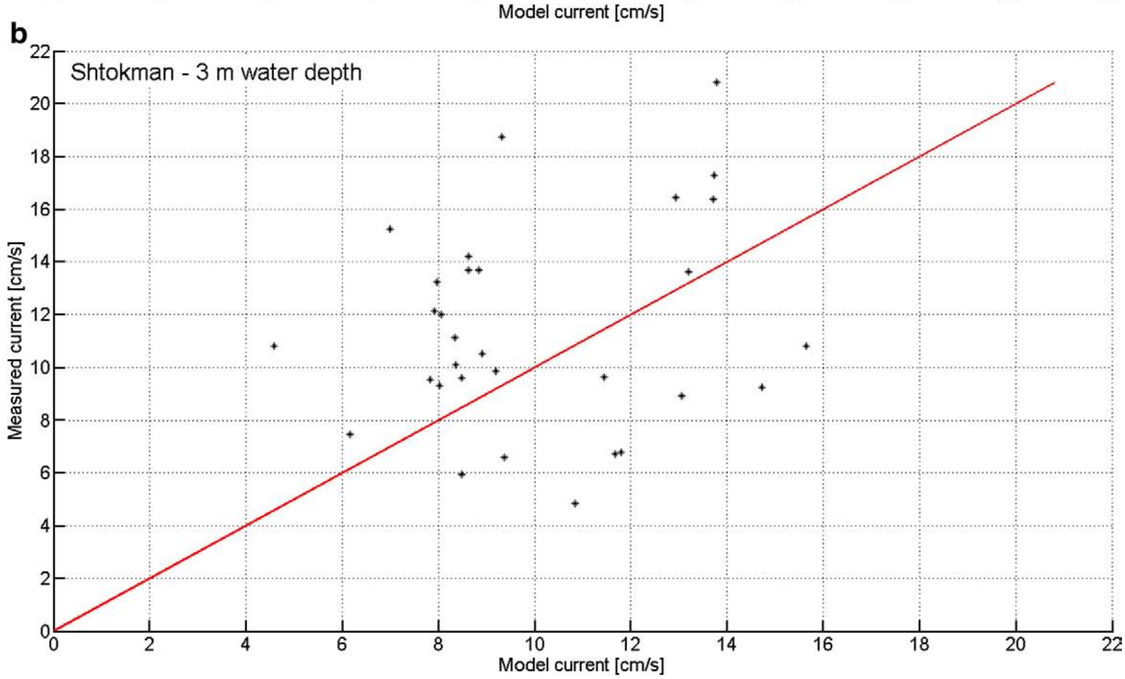

Fig. 7. Scatter diagram showing modified model current speed versus current speed from measurements at 3 m (a and b) and 100 m (c and d) water depth. Scatter a) and c) are based on all recordings in Norwegian sector while b) and d) are from the Shtokman field. Red line shows the equation $y = x$. (For interpretation of the references to color in this figure legend, the reader is referred to the web version of this article.)

axis, minor axis and inclination from model and measurements. The measured amplitudes have been averaged over the measurement depths before the comparison.

4.1.2. Residual currents

For each of the measured records, five types of comparisons with model have been carried out (Table 2). While the first four types of analyses are traditional type of analyses and considered as more or less self-explaining, the trajectory-study needs some further explanation.

The analysis in itself is fairly simple as it is restricted to follow a water particle moving with the speed recorded at the fixed station. With respect to current measurements, typical sampling is 1 h which means that trajectories with 1 h time step may be generated by the recorded datasets. The recorded current value is assumed to be constant both with respect to magnitude and direction throughout the sampling interval. With respect to model currents, the sampling is 1 week[1] which means that model trajectories will be smoother than the measured trajectories. Both sailed distances as well as difference in end position have been stored for each measurement location. The trajectories visualise the quality of the oceanographic

[1] In the iceberg drift model, linear interpolation is used to provide currents with more frequent sampling. In most of the validations of the oceanographic model it has however been preferred to smooth the recordings to get the same sampling interval as the model currents, i.e. 1 week sampling.

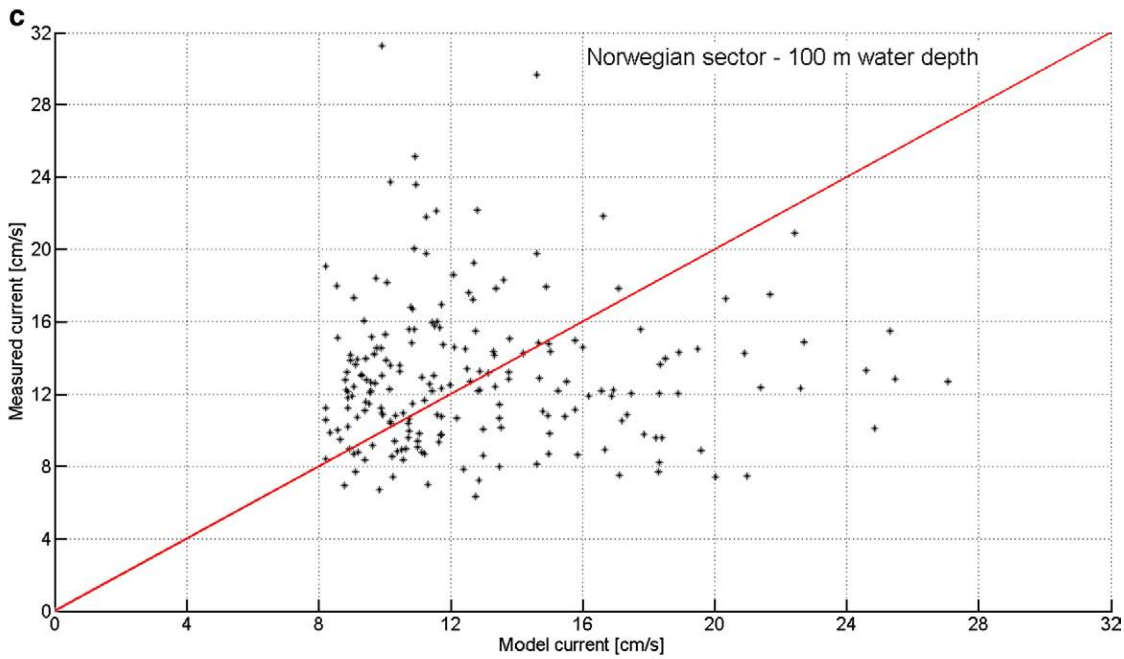

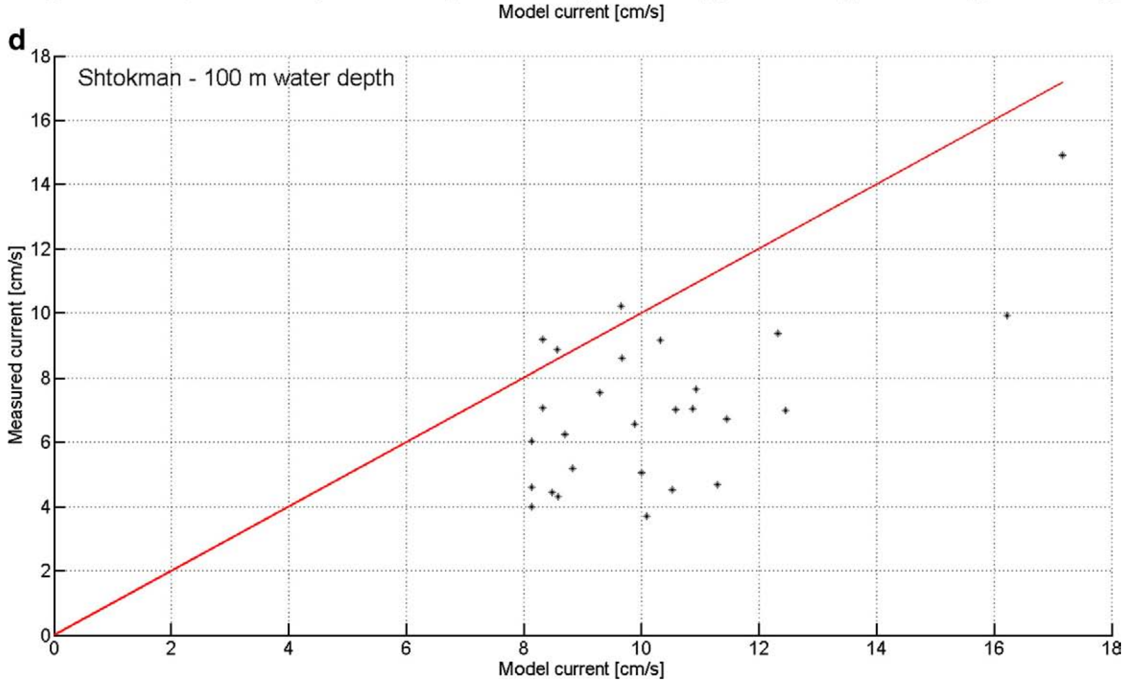

Fig. 7 (*continued*).

model. Only simultaneous model and measurement data have been applied.

With respect to comparisons type 1 to 4 (Table 2), recorded currents were averaged over the exact same weeks as given by the model. All studies revealed that the oceanographic model provides too low currents at all depths and all locations. The differences are illustrated in Fig. 5 for 3 and 100 m water depth at Sentralbanken and Shtokman, respectively. Since bias was more or less constant at all locations a method for correcting the current model was introduced. The methodology for corrections is as follows:

- Statistical distributions (3-parameter Weibull) were fitted to all measured recordings in the Norwegian sector at a certain water depth (3, 50 and 100 m).
- Corresponding distributions were fitted to simultaneous data from the model.
- The hindcast Weibull distribution is adjusted to the measurement distribution by requiring that both distributions shall give equal values for an equal probability level.
- Corrected hindcast current is then expressed by:

$$C_{\mathrm{hc\_cor}} = \left[\frac{C_{\mathrm{hc}} - \varepsilon_{\mathrm{hc}}}{\theta_{\mathrm{hc}}}\right]^{\left(\frac{\gamma_{\mathrm{hc}}}{\gamma_{\mathrm{m}}}\right)} \cdot \theta_{\mathrm{m}} + \varepsilon_{\mathrm{m}} \tag{4}$$

where C_{hc} is current speed from hindcast, $\varepsilon_{\mathrm{hc}}$ and ε_{m} are location parameters in the Weibull distribution for hindcast and measurements, respectively. Correspondingly θ_{hc} and θ_{m} are Weibull scale parameters while γ_{hc} and γ_{m} are Weibull shape parameters. All further results presented in this paper are referring to the modified hindcast currents.

Time series of measured versus modified current speed at Sentralbanken and Shtokman are presented in Fig. 6. An extract of the comparisons are presented in Figs. 7–10. Comparisons that are not included in this paper show similar results as those included herein.

4.2. Meteorological validations

As for currents, simultaneous model and measured winds and waves have been subjected to comparisons both with respect to scatter, magnitude and direction. A representative extract of the results for winds are presented in Figs. 11–14 while corresponding results for waves are presented in Figs. 15–18.

4.2.1. Wind

See Figs. 11 to 14 in pages 17 to 18.

4.2.2. Waves

See Figs. 15 to 18 in pages 18 to 19.

4.2.3. Wind and wave trajectories

In order to investigate the effect of winds and waves on the drift of an iceberg, the iceberg drift model has first been used with only wind speeds as input. Currents have been set constant to zero during the simulations while waves and sea ice have not been included. A tabular shaped iceberg with length 100 m, width 80 m and sail 5 m has been used. Trajectories based on measured and model winds in the same

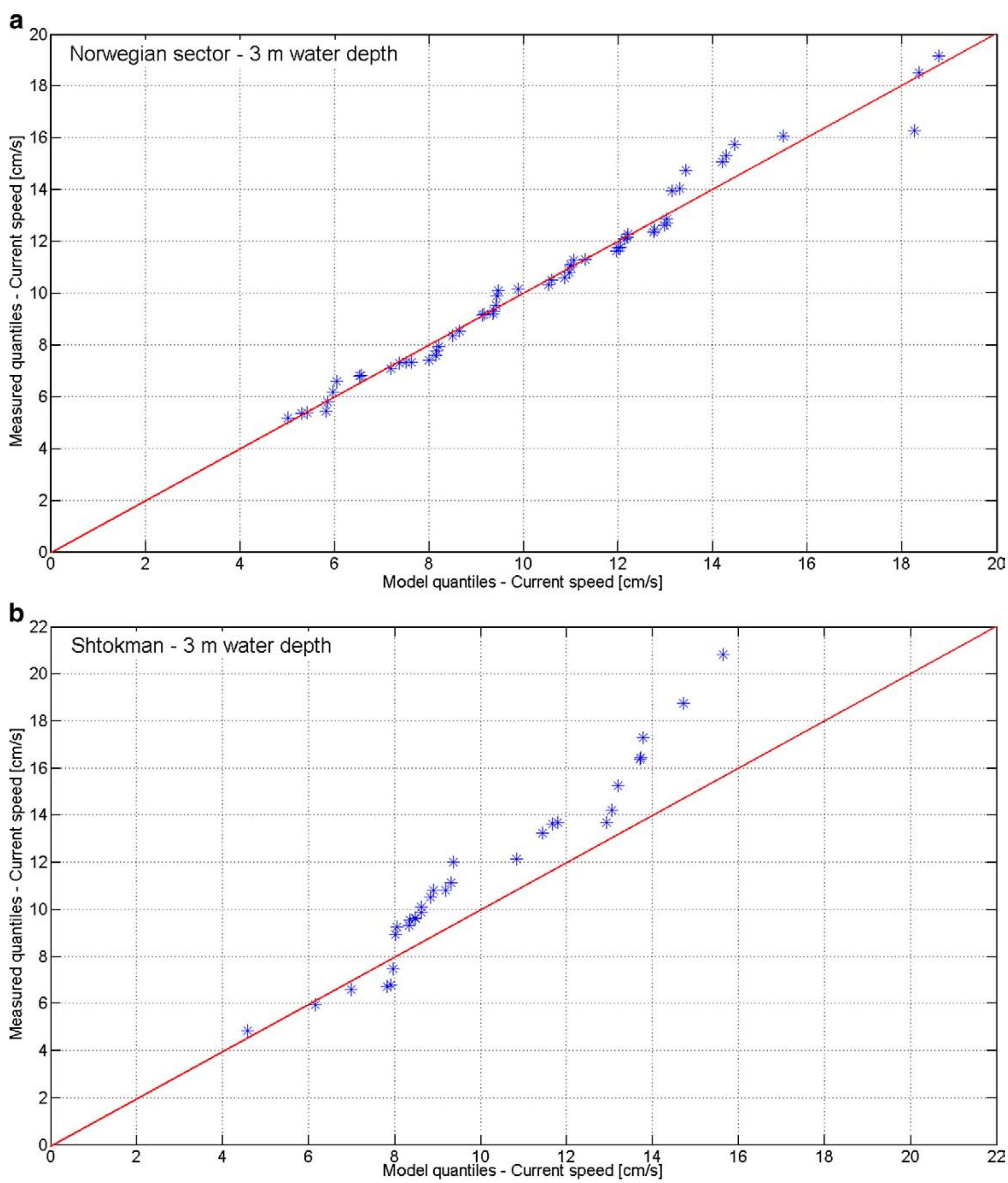

Fig. 8. QQ-plots showing modified model current speed versus current speed from measurements at 3 m (a and b) and 100 m (c and d) water depth. QQ-plot a) and c) are based on all recordings in Norwegian sector while b) and d) are from the Shtokman field. Red line shows the equation $y = x$. (For interpretation of the references to color in this figure legend, the reader is referred to the web version of this article.)

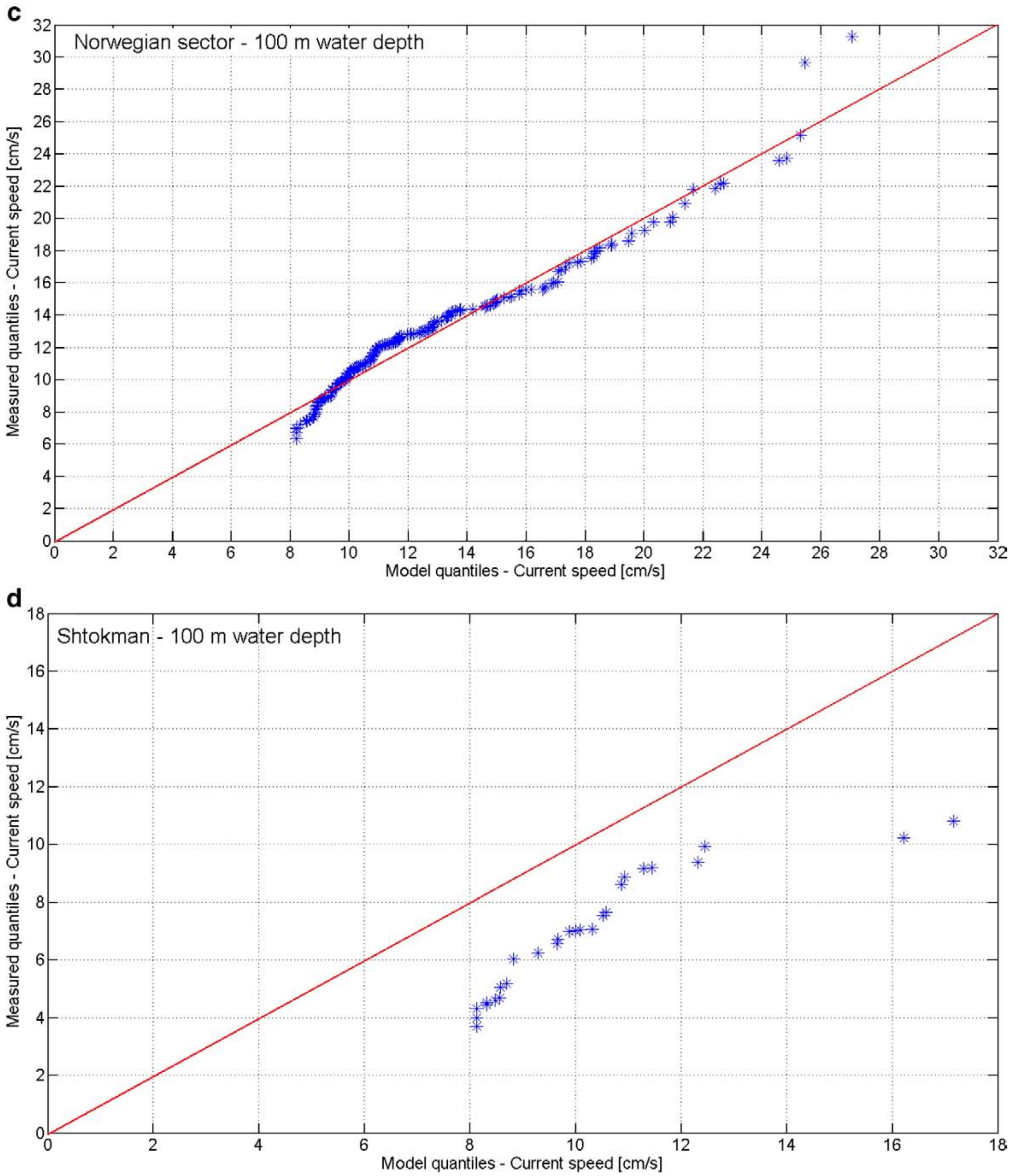

Fig. 8 (*continued*).

plot have been established for all locations where measured winds are available. As some of the datasets span over several years, only some limited periods have been simulated. These periods are the same as the periods with generated current trajectories thus making it possible to compare the effect of winds versus currents on the iceberg drift. Corresponding trajectories for icebergs subjected only to wave forces have also been generated. Representative trajectories are presented in Fig. 19. Formulations for wind and wave forcing are found in Appendix A.

Based on the length of trajectories from simulated icebergs when subjected only to winds, waves or currents, it is possible to provide information regarding the relative importance of each of the parameters. By summing up the length of the trajectories caused by the various forces (wind, waves and currents), the importance of, for example current, is found as the length of the current trajectory divided by the total length. Importance based on the various datasets and corresponding recorded metocean data are presented in Table 3.

4.3. Iceberg drift validations

Trajectories from the model have been compared with totally nine measured trajectories. In light of the quality of underlying metocean data, it was considered meaningful to compare only the three first days of the measured trajectories. Initially, all forcing as described in Section 2 were included. However, two of the trajectories showed that the icebergs were locked into the sea ice during most of the simulation period. As can be seen from Fig. 20 the simulated trajectories show a

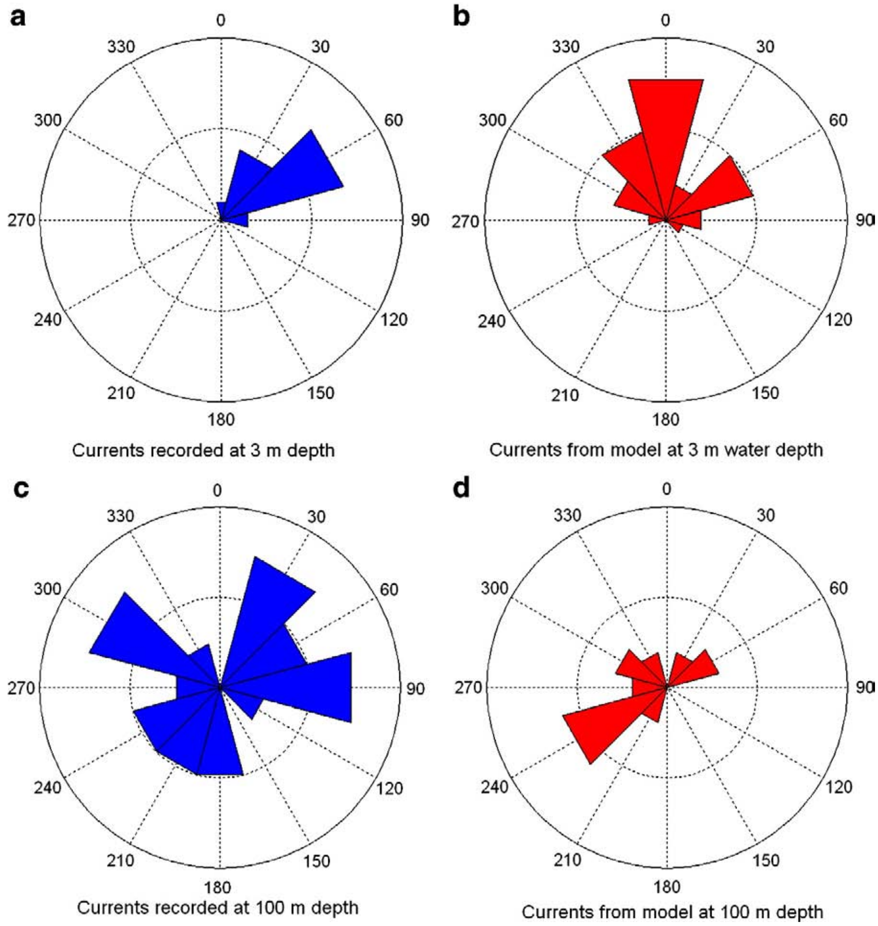

Fig. 9. Directional distributions from measurements (a and c) versus directional distributions from model (b and d) at 3 m and 100 m depth respectively.

poor match to the measured ones. These two icebergs were simulated over again but without including the forces from surrounding sea ice. As can be seen from Fig. 20 the match between simulated and measured trajectories improved significantly when excluding the sea ice drift.

Three of the comparisons between simulated and recorded iceberg drift trajectories are included in Fig. 21. Metocean statistics extracted from the simulations are presented in Table 4. The first trajectory is presented because it shows a fairly good match between recordings and simulations. The second is included because it shows a very good match the first 12 h and that the inertial oscillations are well described. However, this trajectory also illustrates a situation where the model simulates too high drift speed. It should further be noted that forces from surrounding sea ice has been excluded from this particular simulation. The third shows a situation were the simulated iceberg missed the initial drift direction with 90° but which still match the last 24 h of the recordings very well. It should be noted that weekly averaged residual currents were not included in this last simulation.

Despite that only the three first days of each trajectory were used in the comparisons, simulations were also carried out for the full periods with recordings. Average drift speeds and standard deviations based on both simulations and recordings are shown in Table 5.

In order to investigate the importance of wind, waves and currents on iceberg drift, the simulations were repeated with only one of these components included at a time. Based on these simulations, average drift speed due to currents, winds and waves respectively were found. By averaging all speeds from the seven selected IDAP icebergs, it was found that the currents contribute to almost 50% of the total forcing. Corresponding values for wind and waves are presented in Table 6. It should be noted that the IDAP icebergs in significant periods were surrounded by sea ice in various concentrations thus some of the icebergs were not affected by waves at all. With respect to the AARI icebergs, simulations did not include the residual currents thus relative contribution from currents (tide) were much less than for IDAP icebergs. The southernmost AARI trajectory showed, however, that wave forces were equally important as wind.

5. Discussion

With respect to oceanographic data, it is clear that the skills of the applied oceanographic model are far from good. The statistical corrections resulted in a reasonable level for weekly averaged currents both in the eastern as well as the western Barents Sea. However, the usefulness of these data is still limited as the directional information in the oceanographic model also is of poor quality.

The skills of the tidal model may however be considered as good both with respect to magnitude as well as directionality. The tides are considered important in iceberg drift forecasting and in local collision risk analyses. With respect to investigation of long term drift patterns, however, the importance of tidal currents is less important.

The magnitude of wind and waves from the atmospheric and wave models showed good agreement with the recorded data. It could be seen that the model had a tendency to give higher values for high winds compared to the recordings. However, when considering that the majority of recorded winds are from buoys which suffer from sheltering in high sea states, it seems reasonable that model winds are slightly higher. It can also be seen that changes in the wind and waves are well captured at the correct time. With respect to directionality, there is still a need for improvement. In particular, the wave energy in the model is focused in a narrow sector while the recordings show a more spread directionality in the waves.

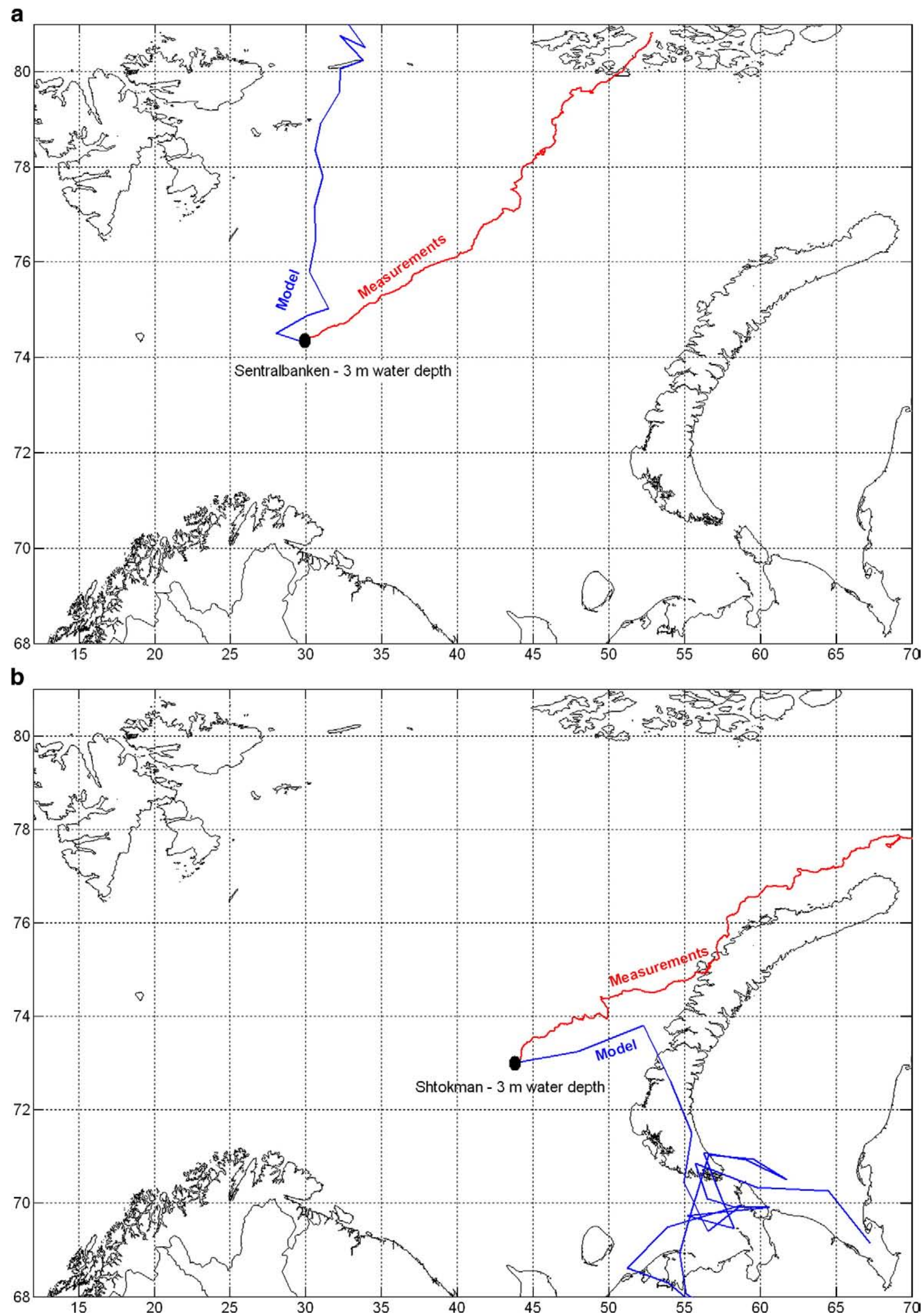

Fig. 10. Trajectories showing displacement of a water particle when subjected to currents from a fixed location spanning over approximately 7 months. Model currents (blue) from 3 m and 100 m versus measured currents (red) from the same depths at Sentralbanken are shown in (a) and (c) respectively. Corresponding values from Shtokman are presented in (b) and (d). (For interpretation of the references to color in this figure legend, the reader is referred to the web version of this article.)

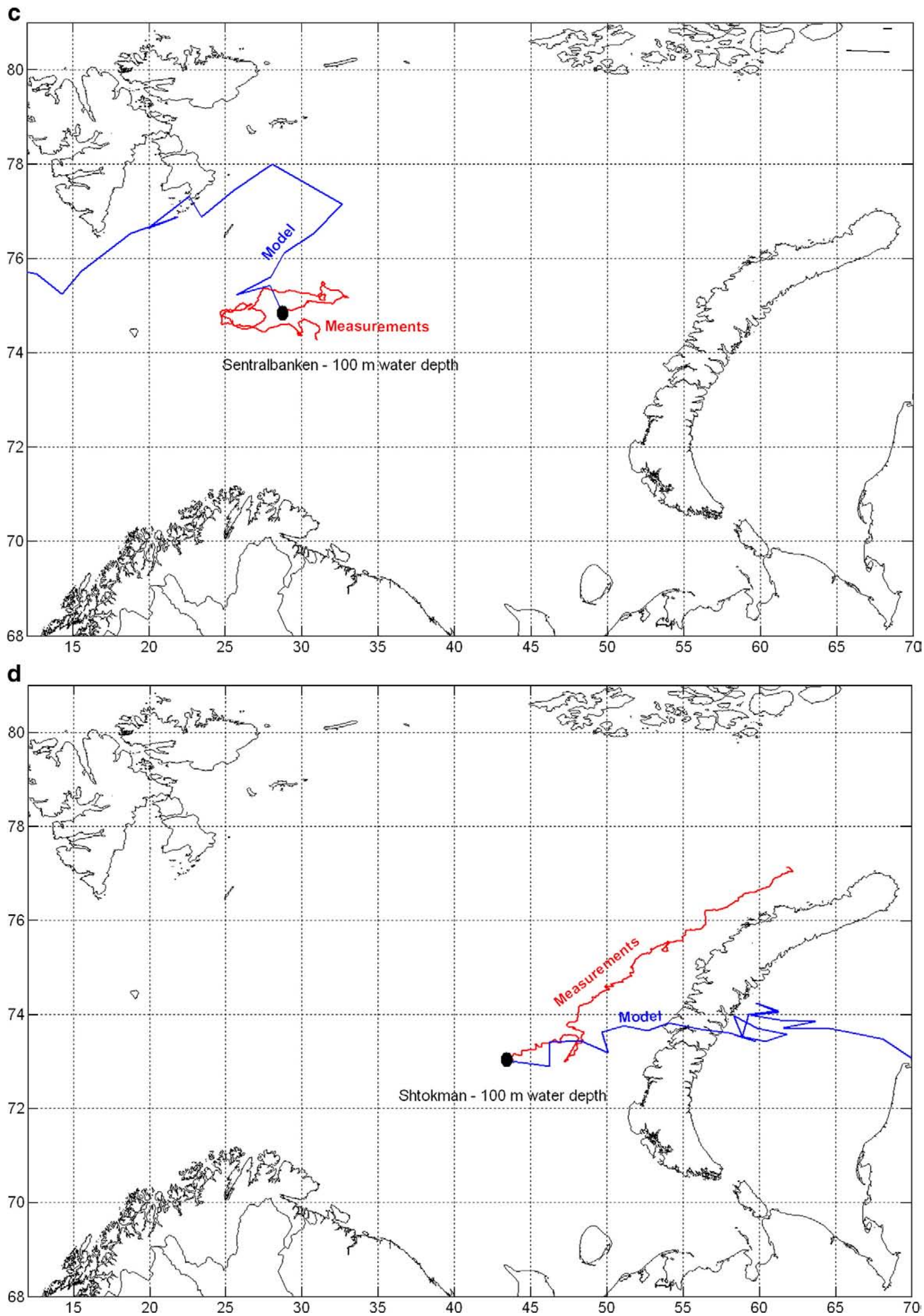

Fig. 10 (*continued*).

As expected, there was no perfect match between simulated and measured trajectories. A few of the simulation could be considered as "disqualifying" if the model where to be applied in a forecasting mode. However, in all of the trajectories, there were clear correspondences between recorded and modelled trajectories. It is evident that changes in the wind conditions were captured well. Further, circular patterns,

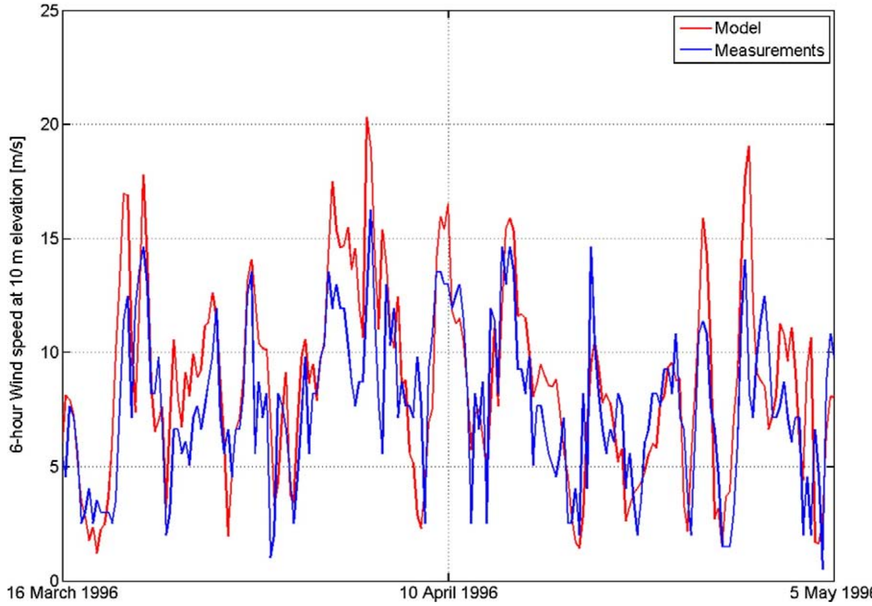

Fig. 11. Extract of time series with measured versus model wind speed at Shtokman.

either due to tidal currents or inertial oscillations seemed to be captured well.

The model does also provide useful information regarding the relative importance of the forces. It is evident that the currents are important, and often the most important parameter in iceberg drifts. In open water, at some distance from the ice edge however, the wave drift forces seem to be more important.

The model shows examples where icebergs get locked in the sea in accordance to the AWI criteria (Lichey and Hellmer, 2001). This happens when the sea ice concentration is higher than 90% and the sea ice strength is sufficiently high. The sea ice strength is formulated as a function of the ice thickness and ice concentration. When an iceberg is locked in the sea ice, it follows the sea ice drift patterns. Trajectories from icebergs, which in accordance to simulations were locked in the sea ice, generally show a very poor match with recorded trajectories. There may be several reasons for this; first of all there is no information whether the physical icebergs were locked into the sea ice or not. Secondly, there is reason to believe that the numerical sea ice drift model, which is coupled to the oceanographic model (Keghouche et al., 2007), does not provide realistic sea ice drift patterns. The third explanation may be that the theoretical formulation from Lichey and Hellmer (2001) is not adequate for iceberg drift in the Barents Sea. The present study has not included validations of the sea ice/iceberg forces thus it is not possible to conclude on this subject. However, validation of sea ice forces on icebergs should be considered for further work on iceberg drift.

The validation studies performed on the underlying metocean models provide important knowledge regarding the skills of the iceberg drift model. In situations with strong winds and high waves, there is reason to expect reliable results from the iceberg drift model. However, when ocean currents are dominating, the model

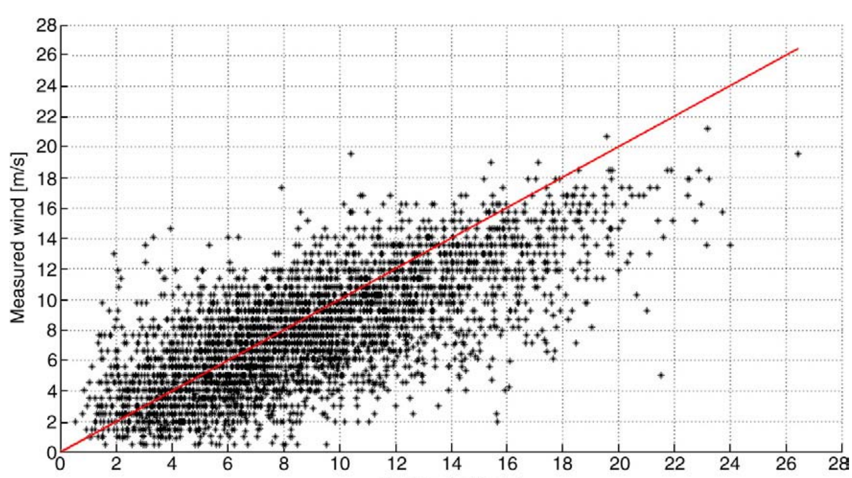

Fig. 12. Scatter diagram showing simultaneous values from measured and model wind speeds. Based on 6 hour averaged winds at Shtokman. Red line shows the equation $y = x$. (For interpretation of the references to color in this figure legend, the reader is referred to the web version of this article.)

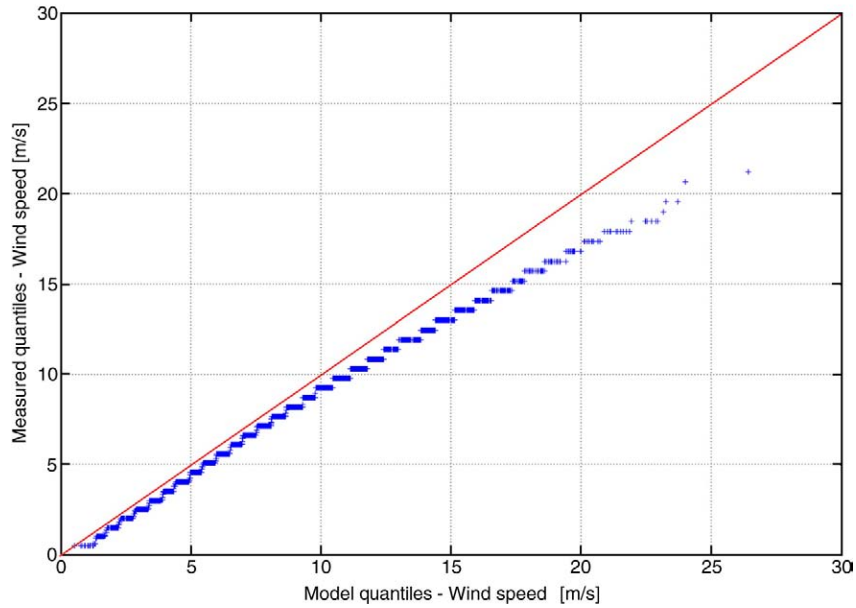

Fig. 13. QQ-diagram showing quantiles from measured and model wind speeds. Based on 6 hour averaged winds at Shtokman. Red line shows the equation $y=x$. (For interpretation of the references to color in this figure legend, the reader is referred to the web version of this article.)

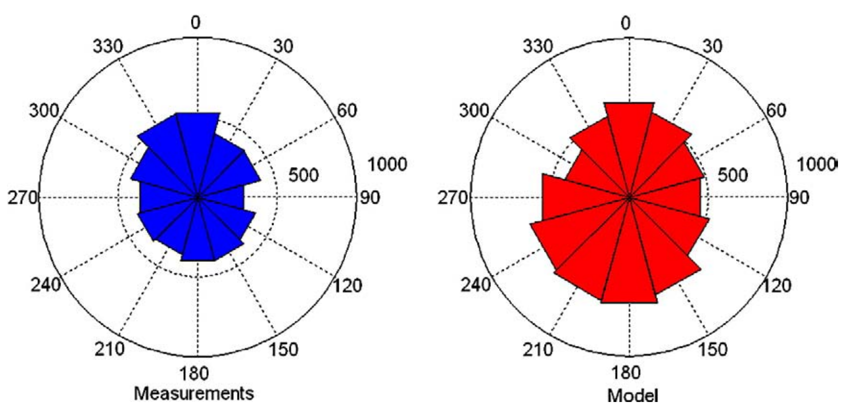

Fig. 14. Comparison of directional distributions from measurements and model at Shtokman. NB! Due to gaps in the measured data set, the model rose is based on more data than the rose representing the measurements.

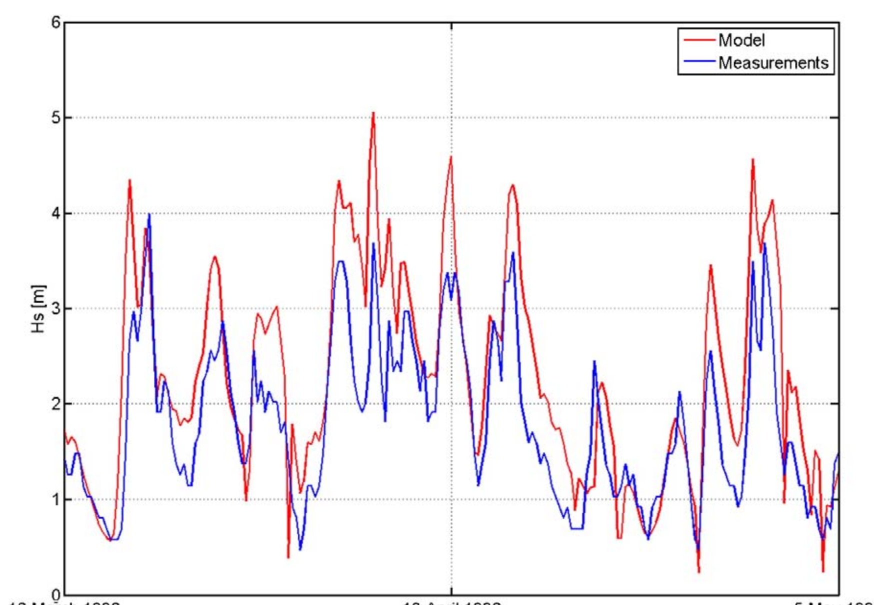

Fig. 15. Extract of time series with measured versus model significant wave height at Shtokman.

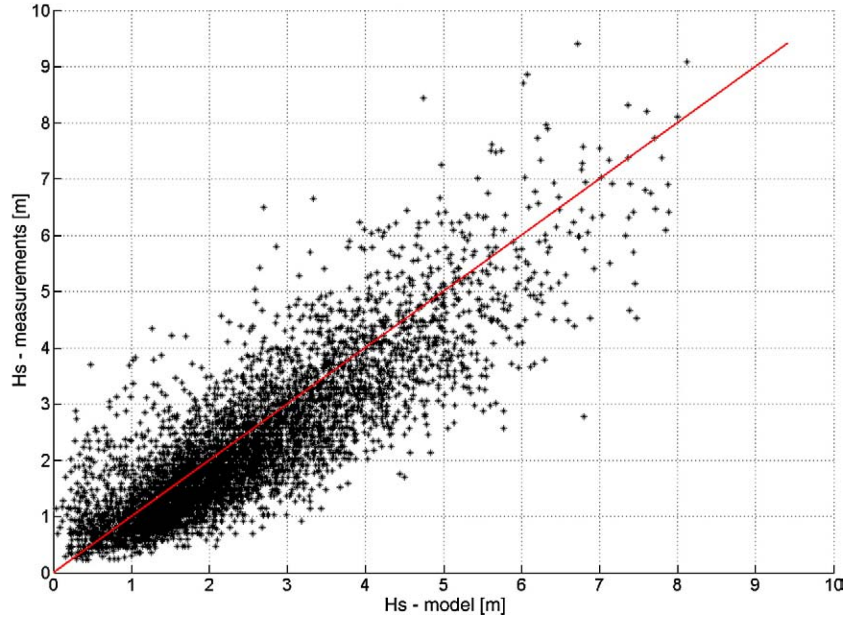

Fig. 16. Scatter diagram showing simultaneous values from measured and model significant wave height at Shtokman. Red line shows the equation $y = x$. (For interpretation of the references to color in this figure legend, the reader is referred to the web version of this article.)

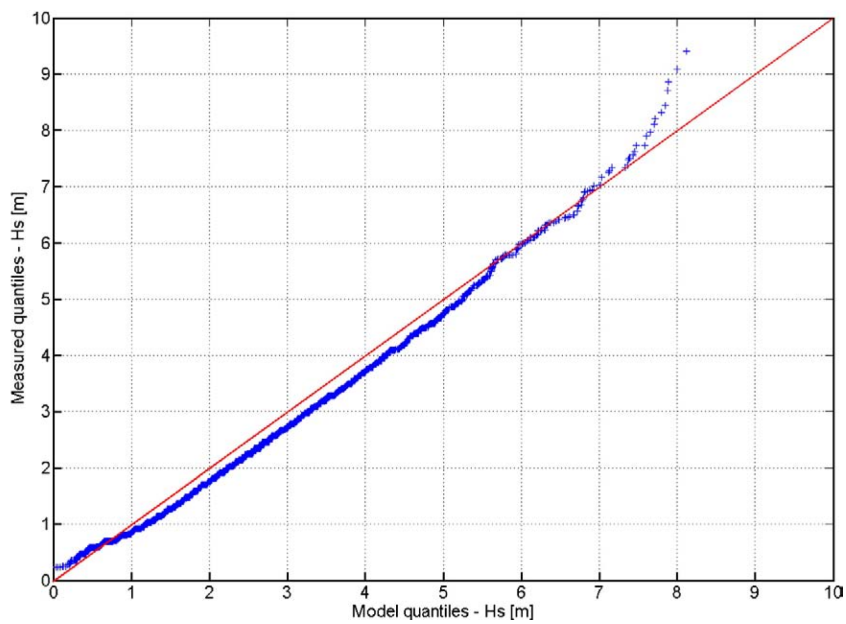

Fig. 17. QQ-diagram showing quantiles from measured and model significant wave height at Shtokman. Red line shows the equation $y = x$.

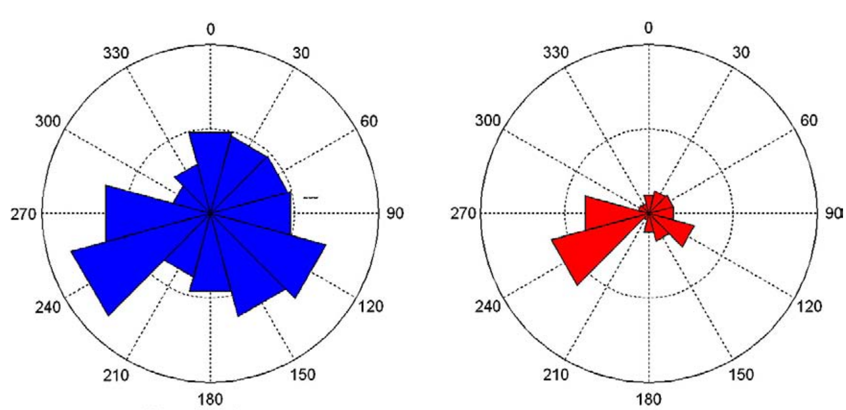

Fig. 18. Comparison of directional distributions from measurements and model at Sentralbanken. NB! Due to gaps in the measured data set, the model rose is based on more data than the rose representing the measurements.

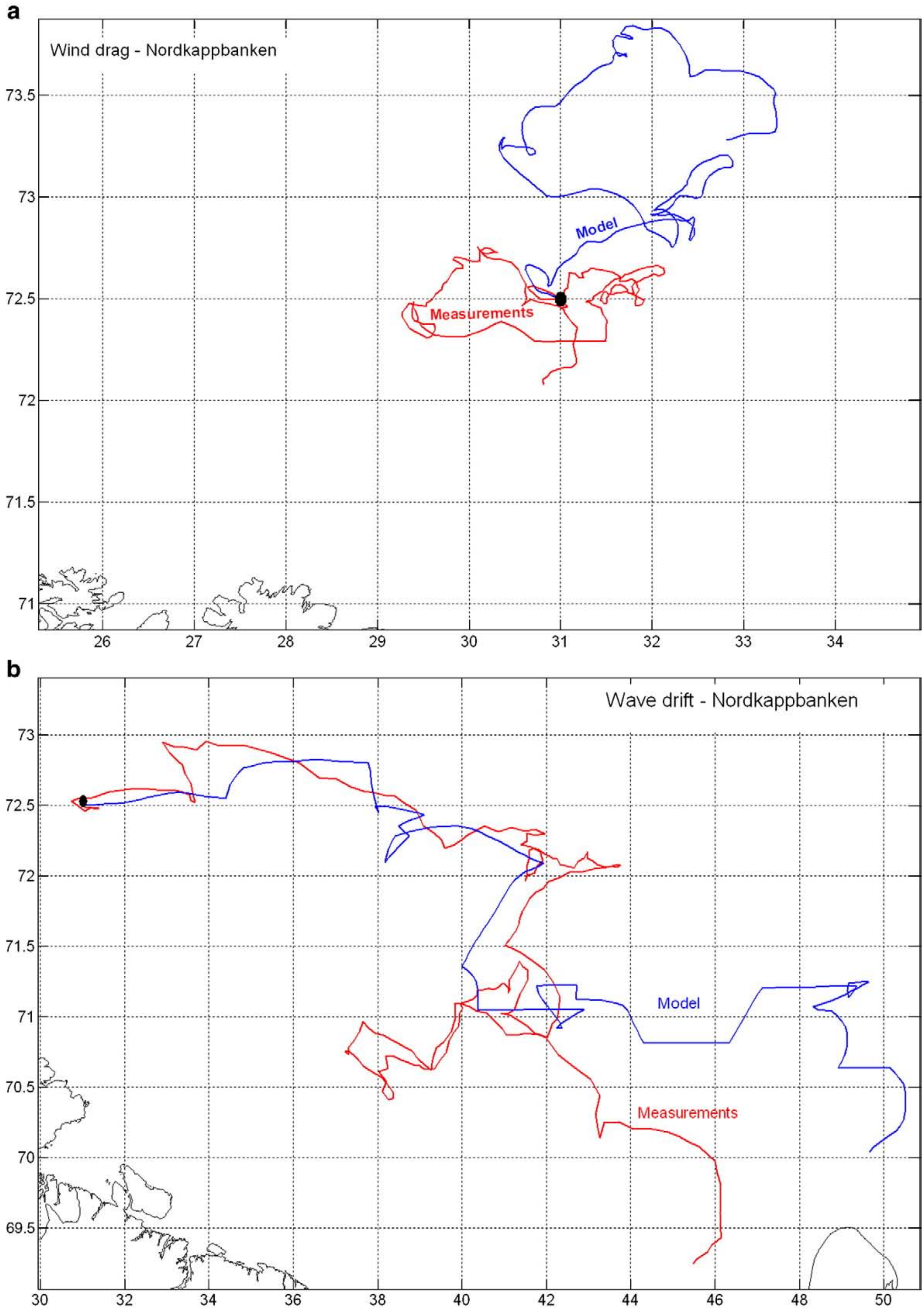

Fig. 19. Iceberg drift trajectories due to forcing from a) wind drag and b) wave drift. Iceberg dimensions (length × width × sail): 100 × 80 × 5 m. Based on recorded data from Nordkappbanken in the period 19.09.1989 to 22.11.1989 and wind/wave data from the Winch hindcast model (Reistad and Iden, 1998) for the same period.

skills may not be satisfactory. In order to ensure a more reliable iceberg drift model further efforts should be given to oceanographic modelling.

Iceberg deterioration has not been treated in this paper. However, it should be noted that iceberg deterioration may affect the iceberg drift significantly. The operational iceberg drift model applied at the East Coast

Table 3
Summary of relative importance and associated metocean parameters.

Data location[a]	Relative importance [%]			Average recorded parameters		
	Currents	Winds	H_s	Currents [cm/s]	Winds [m/s]	H_s [m]
Sentralbanken/OD 1 (3 m depth)	15	19	66	9	8.2	1.9
Bjørnøya/OD 8 (50 m and 100 m depth)	40	12	43	17	5.5	1.5
Nordkappbanken/OD 11 (100 m depth)	25	20	55	12	7.0	2.3
Shtokman (3.5 m depth)	23	17	60	12	6.2	2.0

Based on drift lengths.
[a] Data locations are shown in Fig. 2.

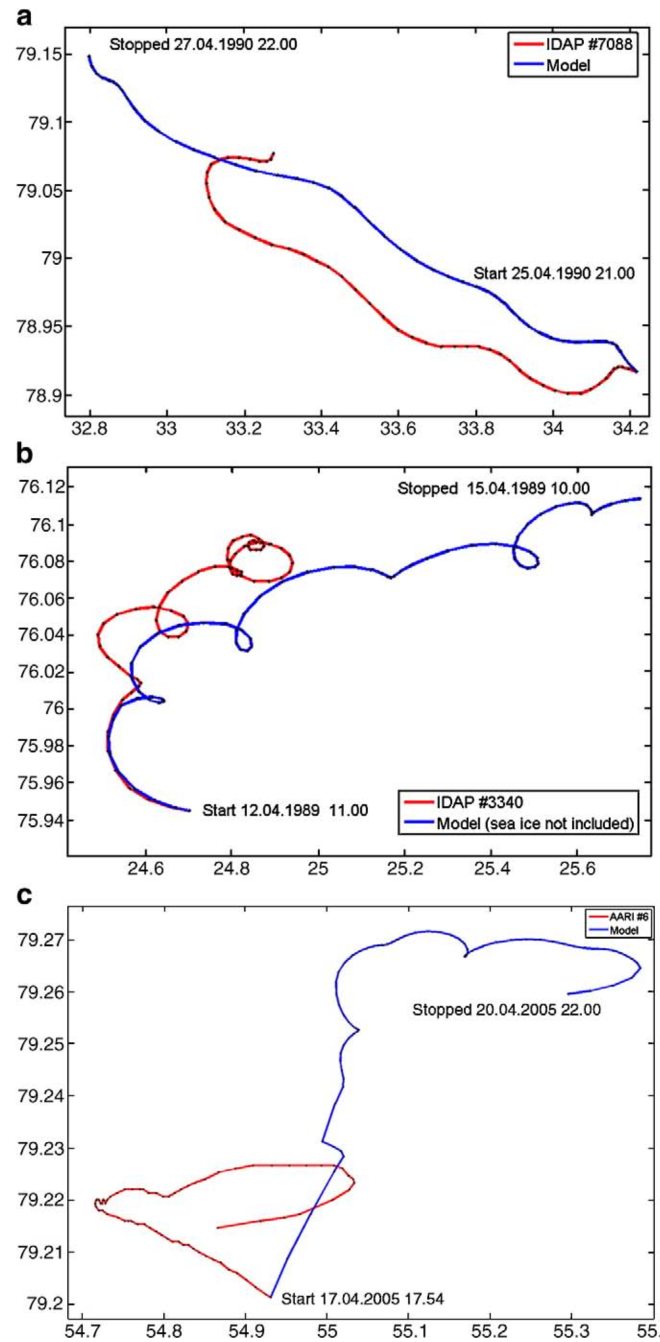

Fig. 21. Selection of comparisons between model and measured iceberg drift trajectories. Start and end of simulation time, which is identical with the first and the last data point in the measured trajectory, are included.

of Canada (Kubat et al., 2007) has been implemented in the presented iceberg drift model. Preliminary simulations indicate that deterioration due to waves in storm situation is significant and that the iceberg drift speed seems to increase as the mass is reduced during the storm.

6. Conclusions

A numerical iceberg drift model for the Barents Sea has been established spanning the period 1987–1992 continuously with wind, wave and current data. The underlying oceanographic and atmospheric models have been subjected to comprehensive validations.

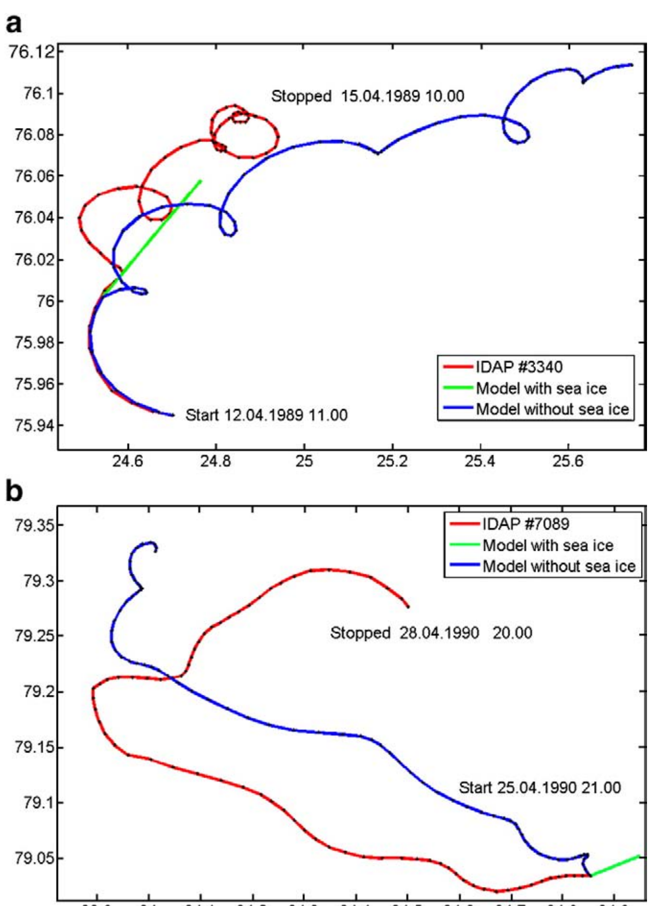

Fig. 20. Plot of two iceberg drift trajectories from recordings (red), simulations including sea ice forces (green) and simulations excluding sea ice forces (blue). (For interpretation of the references to color in this figure legend, the reader is referred to the web version of this article.)

Validations show that both magnitude and directionality in model currents are of poor quality at all locations and at all times in the model domain. A methodology for adjusting the magnitude has successfully been introduced. However, better directional current information must be required from the oceanographic model.

The skills of the atmospheric and wave models are considered good and adequate for iceberg drift modelling. The directionality in both winds and waves may be improved.

Currents are considered as the most important parameter for icebergs drifting in waters close to the ice edge or within the sea ice. In more open water conditions, waves become the most important iceberg drift parameter.

Table 4
Metocean statistics extracted during three iceberg drift simulations.

Parameter	Source	Iceberg buoy number		
		IDAP 3340	IDAP 7088	AARI 6
Current speed [cm/s]	NERSC Barents Sea model	20	12	
	Recordings			
Current direction (towards)	NERSC Barents Sea model	ESE	NW	
	Recordings			
Wind speed [m/s]	Winch model	6.5	10.8	7.1
	Recordings	7.0		
Wind direction (from)	Winch model	SSW	SE	S
	Recordings	SSW		
Sea ice concentration [%]	NERSC Barents Sea model	94	87	
	Recordings	70–90		
Sea ice thickness [m]	NERSC Barents Sea model	1	0.7	
	Recordings	2	1.7	
Sea ice drift speed [cm/s]	NERSC Barents Sea model	4	1	
	Recordings			
Sea ice drift direction (towards)	NERSC Barents Sea model	NE	NNE	
	Recordings			

Iceberg dimensions and start of simulations correspond to size and time for physically recorded trajectories. Recorded ice and metocean conditions are from Løvås et al. (1990) and Jensen et al. (1990). Only mean values based on simulation period (3 days) are included. Empty fields mean that no information on the parameter is found.

Table 5
Statistical characteristics of iceberg drift according to simulations and recordings.

Iceberg buoy no.	Length × width × height	Simulations		Measurements	
		Average speed (cm/s)	Standard deviation (cm/s)	Average speed (cm/s)	Standard deviation (cm/s)
IDAP 3108[a]	80 × 54 × 18	6	2.9	18	
IDAP 3337[a]	65 × 47 × 11	32	11.8	29	
IDAP 3340	80 × 55 × 5	24	12.1	27	
IDAP 7086	90 × 60 × 10	18	8.1	12	
IDAP 7087	63 × 56 × 10	14	8.1	14	
IDAP 7088[a]	95 × 80 × 20	22	9.2	10	
IDAP 7089[a]	95 × 90 × 15	17	8.5	12	
Average IDAP		19	8.7	19	10.0
AARI 6	95 × 63 × 3.7	12	7.4	11	8.2
AARI 8	106 × 70 × 4.5	15	5.2	13	8.3

IDAP recordings are reported by Spring (1994) while AARI recordings are presented in Dmitriev and Nesterov (2007). Note: Some of the simulated trajectories are shorter than recorded trajectories due to grounding in the simulation model.
[a] Simulated iceberg grounded before end of simulation time.

Table 6
Summary of relative importance and associated metocean parameters.

Data location	Relative importance [%]			Average associated values from metocean models		
	Currents	Winds	Waves	Currents [cm/s]	Winds [m/s]	Waves [m]
IDAP (7 icebergs)	49	44	7	17	8.8	0.2
AARI – Franz Josef Land[a]	33	67	0	5	6.6	0.2
AARI – Novaya Zemlya[a]	18	41	41	4	6.6	0.8

Based on forcing in the iceberg drift simulation model.
[a] Only tidal currents were included in addition to wind and waves in the simulations.

Further work, should focus on improvement in oceanographic models for the Barents Sea.

Appendix A. Specifications for iceberg drift model

Expression for drag forces due to wind ($\mathbf{F}_a$) and current ($\mathbf{F}_w$) (Bigg et al., 1997):

$$\mathbf{F}_{a,w} = \rho_{a,w} \cdot C_{a,w} \cdot A_{a,w} \cdot |\mathbf{V}_{a,w} - \mathbf{V}_i| \left(\mathbf{V}_{a,w} - \mathbf{V}_i\right) \tag{A1}$$

Expression for wave drift forces based on potential theory (Faltinsen, 1990):

$$\mathbf{F}_r = \frac{1}{4}\rho_w \cdot g \cdot a^2 \cdot L \cdot \frac{\mathbf{V}_{wa}}{|\mathbf{V}_{wa}|} \tag{A2}$$

Expression for sea ice forces ($\mathbf{F}_i$) (Lichey and Hellmer, 2001):

$$\mathbf{F}_{si} = \begin{cases} 0 & : A \leq 15\% \\ \frac{1}{2}\rho_{si} C_{si} A_{si} |\mathbf{V}_{si} - \mathbf{V}_i| (\mathbf{V}_{si} - \mathbf{V}_i) & : 1 \geq 5\% < A < 90\% \\ -\left(\mathbf{F}_a + \mathbf{F}_w + \mathbf{F}_p + \mathbf{F}_{cor}\right) & : A \geq 90\% \text{ and } h \geq h_{min} \end{cases} \tag{A3}$$

Expression for pressure gradient force ($\mathbf{F}_p$) (Kubat et al., 2005)

$$\mathbf{F}_p = m\left(\frac{d\mathbf{V}_{mw}}{dt} + \mathbf{f} \times \mathbf{V}_{mw}\right) \tag{A4}$$

Expression for Coriolis force ($\mathbf{F}_{cor}$) (Bigg et al., 1997):

$$\mathbf{F}_{cor} = -m \cdot \mathbf{f} \times \mathbf{V}_i \tag{A5}$$

Table A1
Parameter descriptions.

Parameter	Description	Recommended value	Reference
ρ_a	Air density	1.225 [kg/m^3]	
ρ_w	Water density	1027 [kg/m^3]	
ρ_{si}	Sea ice density	900 [kg/m^3]	
C_a	Air drag coefficient	1.3 [−]	Bigg et al. (1997)
C_w	Water drag coefficient	0.9 [−]	Bigg et al. (1997)
C_{si}	Sea Ice drag coefficient	1.0 [−]	Lichey and Hellmer (2001)
A_a	Cross sectional area above the water surface and normal to the wind speed	iceberg—sail $\cdot \frac{\text{width} + \text{length}}{2}$	
A_w	Cross sectional area below the surface and normal to the wind speed	$7.1 \cdot \text{sail} \cdot \frac{\text{width} + \text{length}}{2}$	
A	Sea ice concentration	From ice-ocean model	Keghouche et al. (2007)
V_a	Wind velocity	From Winch model	Reistad and Iden (1998)
V_w	Current velocity	From ice-ocean model	Keghouche et al. (2007)
V_i	Iceberg velocity	Calculated	
V_{si}	Sea ice velocity	From ice-ocean model	Keghouche et al. (2007)
V_{mw}	Mean water current velocity	Current velocity averaged over the iceberg draft is applied	
g	Gravity	9.81 [m/s^2]	
a	Wave amplitude	$\frac{1}{2} \cdot H_s$	Faltinsen (1990)
H_s	Significant wave height (average height of the 1/3 highest waves in a sea state)	From Winch model	Reistad and Iden (1998)
C_w	Wave drift force coefficient	0.6 [−]	Isaacson (1988)
$\frac{V_{wa}}{\lvert V_{wa}\rvert}$	Wave direction	From Winch model	Reistad and Iden (1998)
L	Iceberg length		
m	Iceberg mass	Physical mass + added mass = 1.5 times the physical mass	Kubat et al. (2005)
h	Sea ice thickness		
h_{min}	Minimum ice thickness needed to lock an iceberg in the sea ice	$h_{min} = \frac{P}{P^* \exp[-20(1-A)]}$	Lichey and Hellmer (2001)
P	Sea ice strength	Average 660.9 [N/m]	Lichey and Hellmer (2001)
P^*	Sea ice coefficient	20,000 [N/m^2]	Lichey and Hellmer (2001)

Appendix B. Time spans of Barents Sea metocean measurements

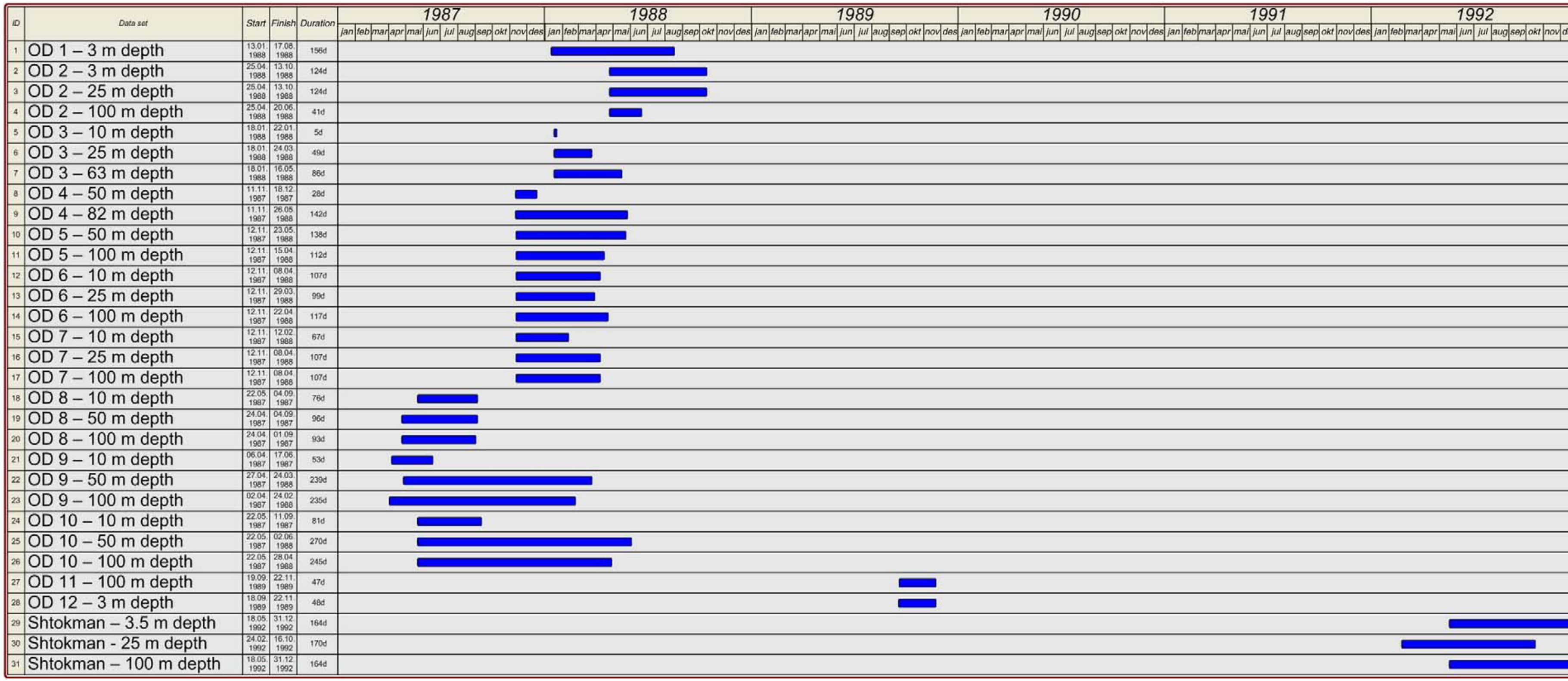

Fig. B1. Time spans of Barents Sea current measurements.

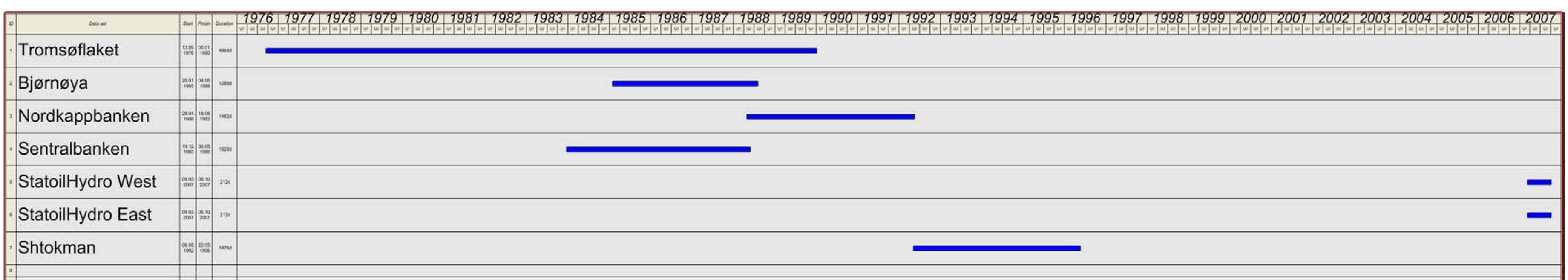

Fig. B2. Time spans of Barents Sea wind and wave measurements.

References

Bigg, G.R., Wadley, M.R., Stevens, D.P., Johnson, J.A., 1997. Modelling the dynamics and thermodynamics of icebergs. Cold Regions Science and Technology 26, 113–135.

Dmitriev, N. Ye, Nesterov, A.V., 2007. Iceberg drift in the Barents sea according to observation data and simulation results. Proceedings 17th International Offshore and Polar Engineering Conference, ISOPE'07, Lisbon, Portugal, pp. 633–638.

Faltinsen, O.M., 1990. Sea Loads on Ships and Offshore Structures. Cambridge University Press, Great Britain.

Foreman, M.G.G., 1978. Manual for tidal currents, analysis and prediction. Institute of Ocean Sciences, Patricia Bay, Sidney, BC Canada. Pacific Marine Science Report 78-6. revised October 2004.

Gjevik, B., Straume, T., 1998. Simulations of the M2 and K1 tide in the Nordic Seas and the Arctic Ocean. Tellus, Ser. A, vol. 41, pp. 73–96.

Gjevik, B., Nøst, E., Straume, T., 1994. Model simulations of the tides in the Barents Sea. Journal of Geophysical Research 99, 3337–3350.

Isaacson, M., 1988. Influence of Wave Drift Force on Ice Mass Motions. Proceedings 7th International Conference on Offshore Mechanics and Arctic Engineering (OMAE), vol. 2, pp. 125–130.

Jensen, H., Løvås, S.M., Vinje, T., Løyning, T., 1990. B IDAP 90 R/V Lance Deployment. Field observations and analysis, vol. 2. Report from the Ice Data Acquisition Programme (IDAP), Sintef project 604872, 82 pp.

Johannessen, K., Løset, S., Strass, P., 1999. Simulation of iceberg drift. Proceedings 15th International conference on Port and Ocean Engineering under Arctic Conditions, POAC'99, Helsinki, Finland, pp. 97–105.

Keghouche, I., Bertino, L., Sandven, S., 2007. Iceberg modelling in the Barents Sea: Part I, initial Tests. NERSC Tech. Rep. 280.

Kleiven, G., Meisingset, H.C., 2003. Analysis of metocean data from the Shtokman Area. Norsk Hydro report NH-00199965.

Kubat, I., Sayed, M., Savage, S.B., Carrieres, T., 2005. An operational model of iceberg drift. International Journal of Offshore and Polar Engineering 15 (2), 125–131 ISSN 1053–5381.

Kubat, I., Sayed, M., Savage, S.B., Carrieres, T., Crocker, G., 2007. An operational iceberg deterioration model. Proceedings of 17th International Offshore and Polar Engineering Conference, ISOPE'07, Lisbon, Portugal, pp. 652–657.

Lichey, C., Hellmer, H.H., 2001. Modeling giant-iceberg drift under the influence of sea ice in the Weddell Sea. Antarctica, Journal of Glaciology 47 (158), 452–460.

Løvås, S.M., Løyning, T.B., Jensen, H., Johnsen, Å., 1990. IDAP 90 R/V Lance Deployment. Re-analysis of Iceberg drift data from 1988 and 1989, vol. 3. Report from the Ice Data Acquisition Programme (IDAP), Sintef project 604872, 100 p.

The Mathworks, 2008. Matlab Function Reference. Website: http://www.mathworks.com/access/helpdesk/help/techdoc/index.html?/access/helpdesk/help/techdoc/ref/ode113.html&http://www.mathworks.com/cgi-bin/texis/webinator/search/?db=MSS&prox=page&rorder=750&rprox=750&rdfreq=500&rwfreq=500&rlead=250&sufs=0&order=r&is_summary_on=1&ResultCount=10&query=ODE15s&submitButtonName=Search [cited 1 September 2007].

Oceanor, 1998. Innsamling av naturdata i Norskehavet og Barentshavet, Sammendrag 1976–1997. Summary report OCN R-98038 delivered to Norwegian Petroleum Directorate (NPD) 1998.

Reistad, M., Iden, K., 1998. Updating, correction and evaluation of a hindcast data base of air pressure, wind and waves for the North Sea, the Norwegian Sea and the Barents Sea. Norwegian Meteorological Institute, Research report No. 9, 1998.

Spring, W., 1994. Ice Data Acquisition Summary Report. Mobil Research and Development Corporation, Texas, US.